catalysts

MDPI

Review

Oxidative Degradation of Pharmaceuticals: The Role of Tetrapyrrole-Based Catalysts

Giusi Piccirillo, Rafael T. Aroso, Fábio M. S. Rodrigues, Rui M. B. Carrilho, Sara M. A. Pinto, Mário J. F. Calvete * and Mariette M. Pereira *

Department of Chemistry, University of Coimbra, Rua Larga, 3004-535 Coimbra, Portugal; giupiccirillo12@gmail.com (G.P.); rafael.aroso@student.uc.pt (R.T.A.); fmsrodrigues.qui@gmail.com (F.M.S.R.); rui.carrilho@uc.pt (R.M.B.C.); smpinto@qui.uc.pt (S.M.A.P.)

* Correspondence: mcalvete@qui.uc.pt (M.J.F.C.); mmpereira@qui.uc.pt (M.M.P.)

Abstract: Nowadays, society's widespread consumption of pharmaceutical drugs and the consequent accumulation of such compounds or their metabolites in effluents requires the development of efficient strategies and systems that lead to their effective degradation. This can be done through oxidative processes, in which tetrapyrrolic macrocycles (porphyrins, phthalocyanines) deserve special attention since they are among the most promising degradation catalysts. This paper presents a review of the literature over the past ten years on the major advances made in the development of oxidation processes of pharmaceuticals in aqueous solutions using tetrapyrrole-based catalysts. The review presents a brief discussion of the mechanisms involved in these oxidative processes and is organized by the degradation of families of pharmaceutical compounds, namely antibiotics, analgesics and neurological drugs, among others. For each family, a critical analysis and discussion of the fundamental roles of tetrapyrrolic macrocycles are presented, regarding both photochemical degradative processes and direct oxidative chemical degradation.

Keywords: tetrapyrrolic macrocycle; porphyrin; phthalocyanine; antibiotics; pharmaceuticals; degradation; photodegradation; heterogeneous; oxidation

Citation: Piccirillo, G.; Aroso, R.T.; Rodrigues, F.M.S.; Carrilho, R.M.B.; Pinto, S.M.A.; Calvete, M.J.F.; Pereira, M.M. Oxidative Degradation of Pharmaceuticals: The Role of Tetrapyrrole-Based Catalysts. *Catalysts* **2021**, *11*, 1335. https://doi.org/10.3390/catal11111335

Academic Editors: Kotohiro Nomura, Alfonso Grassi, Martin Kotora, Takeshi Ohkuma, Victorio Cadierno, Carmine Capacchione, Ken-ichi Fujita, Raffaella Mancuso, Armando Pombeiro, Fabio Ragaini, Carl Redshaw and Kei Manabe

Received: 8 October 2021
Accepted: 1 November 2021
Published: 4 November 2021

1. Introduction

The increasing presence of pharmaceuticals in wastewaters has become a huge environmental problem due to direct toxicity to living organisms and particularly the development of antibiotic-resistant bacteria. Therefore, it is urgent to develop processes capable of destroying these drug-based pollutants in the environment. Among the multiple oxidative processes described in the literature so far [1–7], this review intends to cover exclusively the ones based on the use of tetrapyrrolic macrocycle (TPM) catalysts over the last decade. First, for systematic-mechanistic clarification, we present the accepted photo- and non-photo oxidation mechanisms, and the following sections are focused on the photochemical and non-photochemical degradation of several families of pharmaceutical drugs using TPM-based catalysts.

Oxidation Mechanisms Using Tetrapyrrolic Macrocycle-Based Catalysts

The general photochemical mechanism involved in the degradation of pharmaceutical drugs using photosensitizers, such as tetrapyrrolic macrocycles, is depicted in Scheme 1.

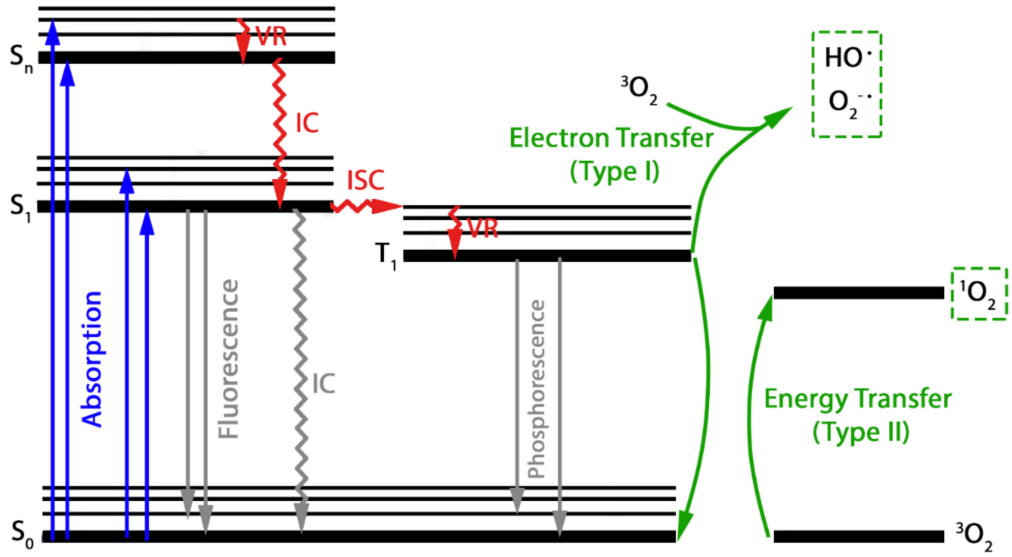

Scheme 1. Adapted Jablonski diagram depicting the relevant electronic transitions that promote ROS formation in photocatalysis (in green), corresponding deactivating mechanisms (in gray) and other radiationless processes (in red): VR = vibrational relaxation; IC = internal conversion; ISC = intersystem crossing.

The absorption of visible light with an appropriate wavelength promotes the catalyst/photosensitizer excitation from the singlet ground state, S_0, to a singlet excited state (S_1, S_2, ... S_n). Generally, if a transition occurs to singlet excited states of a higher order (S_2 to S_n), a quick transition to S_1 occurs through vibrational relaxation (VR) and internal conversion (IC). Singlet excited states are short-lived and can directly return to the ground state through fluorescence emission or IC. Alternatively, an intersystem crossing (ISC) can occur to a triplet excited state (usually T_1), which is a longer-lived state capable of interacting with oxygen under two mechanisms. On the one hand, a direct or indirect electron transfer to molecular oxygen can occur (Type I mechanism), ultimately resulting in the formation of $HO^{\bullet}$ and/or $O_2^{\bullet-}$. On the other hand, an energy transfer (Type II mechanism) can occur between the catalyst in T_1 and $^3O_2$, resulting in the concomitant return of the catalyst to the ground state (S_0) and the formation of singlet oxygen ($^1O_2$) [8,9].

For Type I reactions [10], the photosensitizer (PS) in the triplet excited state ($^3PS^*$) can directly interact with substrates present in the medium to original either anionic or cationic radical species ($PS^{\bullet-}$ and/or $PS^{\bullet+}$; Equations (1) and (2)). In particular, the anionic species $PS^{\bullet-}$ can interact with molecular oxygen, forming superoxide anion ($O_2^{\bullet-}$), while returning to its ground state (Equation (3)). Then, the reversible protonation of $O_2^{\bullet-}$ can lead to the formation of peroxo radicals ($HOO^{\bullet}$; Equation (4)), which can then combine and form H_2O_2 (Equation (5)). Finally, the reaction of H_2O_2 with $O_2^{\bullet-}$ can lead to the formation of $HO^{\bullet}$ (Equation (6)), which is considered the most reactive ROS as it possesses a higher one-electron redox potential and thus can oxidize a wider number of substrates [9].

$$^3PS^* + Substrate \rightarrow PS^{\bullet-} + Substrate^{\bullet+} \quad (1)$$

$$^3PS^* + Substrate \rightarrow PS^{\bullet+} + Substrate^{\bullet-} \quad (2)$$

$$PS^{\bullet-} + O_2 \rightarrow PS + O_2^{-} \quad (3)$$

$$O_2^{\bullet-} + H_2O \leftrightarrow HOO^{\bullet} + HO^{-} \quad (4)$$

$$2\,HOO^{\bullet} \rightarrow H_2O_2 + O_2 \quad (5)$$

$$O_2^{\bullet-} + H_2O_2 \rightarrow O_2 + HO^{\bullet} + HO^{-} \quad (6)$$

In the cases where there is a presence of either free Fe^{3+}/Fe^{2+} or the corresponding metal tetrapyrrolic macrocycles complexes [11], a Fenton-type redox reaction of H_2O_2 with Fe^{2+} can occur, leading to the formation of more $OH^{\bullet}$ (Equation (7)). The reaction of the formed Fe^{3+} with $O_2^{\bullet-}$ can regenerate the active Fe^{2+} species (Equation (8)).

$$H_2O_2 + Fe^{2+} \rightarrow HO^{\bullet} + HO^{-} + Fe^{3+} \quad (7)$$

$$O_2^{\bullet-} + Fe^{3+} \rightarrow O_2 + Fe^{2+} \quad (8)$$

Additionally, Fenton-type redox reactions can also occur with peroxymonosulfate (PMS) to generate sulfate radicals, also commonly used in several advanced oxidation processes (AOPs). Radiation, such as UV, can efficiently activate PMS. Two activation pathways might occur when using radiation. The first one is the O-O bond fission provoked by the input of energy (Equations (9) and (10)). Furthermore, the radiation might dissociate water molecules (Equation (11)), producing the electron, which activates PMS by electron conduction (Equations (12) and (13)) [12].

$$S_2O_8^{2-} \xrightarrow{h\nu} 2\,SO_4^{\bullet-} \quad (9)$$

$$HSO_5^{-} \xrightarrow{h\nu} SO_4^{\bullet-} + HO^{\bullet} \quad (10)$$

$$H_2O \xrightarrow{h\nu} H^{\bullet} + HO^{\bullet} \quad (11)$$

$$S_2O_8^{2-} + H^{\bullet} \rightarrow SO_4^{\bullet-} + SO_4^{2-} + H^{+} \quad (12)$$

$$HSO_5^{-} + H^{+} \rightarrow SO_4^{\bullet-} + H_2O \quad (13)$$

For pharmaceutical degradation, the ideal outcome of ROS-promoted degradation would be the total mineralization of the products, as depicted in Equation (14).

$$ROS + Drug \rightarrow CO_2 + H_2O \quad (14)$$

It is worth noting that tetrapyrrole-based catalysts for photodegradation are often used in hybrid materials containing semiconductors in order to take advantage of their absorption in the UV region and complementary mechanisms of ROS formation. These are summarized in Scheme 2.

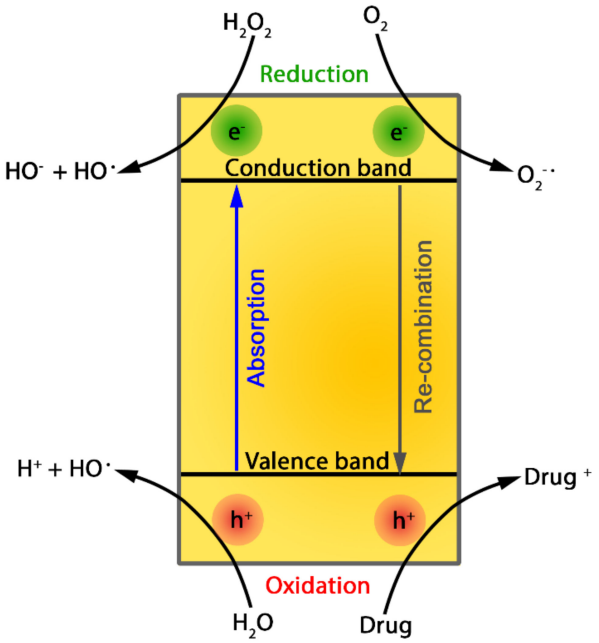

Scheme 2. General mechanism for ROS formation using semiconductors.

Light absorption by semiconductors promotes charge dissociation, resulting in the formation of positively charged holes (h^+) in the valence band (VB) and electrons (e^-) in the conduction band (CB). Positively charged holes can promote oxidation reactions of organic molecules (drugs) adsorbed on the surface of the catalyst or generate ROS via water conversion into $HO^\bullet$. On the other hand, electrons in the CB can be transferred to molecular oxygen, generating $O_2^{\bullet -}$, or promote reduction in H_2O_2 to $HO^\bullet$. These semiconductor-promoted oxidation mechanisms are complementary to the ROS formation pathways mentioned above for the TPM-based catalysts and thus potentiate drug degradation. [1,13] Thus, a significant portion of the work developed in this field has been focused on the development of hybrid catalysts comprising TPM immobilized in semiconductors [2,14–22].

In the absence of light, metal complexes of tetrapyrrolic macrocycles can also promote substrate oxidation in the presence of oxidants such as O_2 or H_2O_2. In fact, this process plays a crucial role in human drug metabolism, where the heme group containing a Fe(II)/Fe(III) metalloporphyrin is the prosthetic group of the cytochrome P450, one of the most important oxidative enzyme families [23–26]. Typically, biomimetic drug degradation studies for environmental remediation use water as a matrix, H_2O_2 as the oxidant and a simplified mechanism, as depicted in Scheme 3. The first step involves the coordination of the central metal with H_2O_2 and the formation of a peroxo species. It is worth mentioning that in cases where O_2 is used as an oxidant, there are two additional reductive steps to activate it in order to form the peroxo species. Then, the formation of oxo species occurs after H_2O elimination and oxidation of the central metal [27,28]. In protic solvents, these intermediates can then react with drugs and promote a series of oxidative reactions, namely epoxidations, hydroxylation, dealkylation, deamination, decarbonylation, N- or S-oxidation, among others [29].

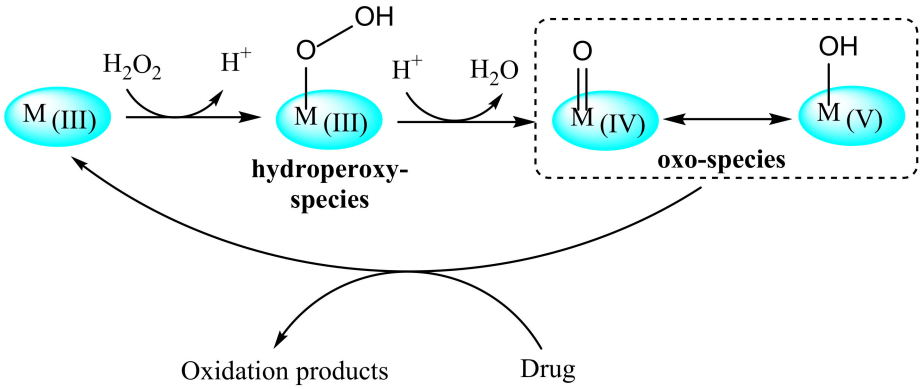

Scheme 3. Simplified mechanism for drug oxidation using H_2O_2 and a tetrapyrrolic-based metal complex.

2. Degradation of Antibiotics

The term antibiotic derives from the ancient greek *αντί* (anti) + βιοτικός (biotikos), which means "against a living being". Therefore, these drugs are exclusively used to treat bacterial infections and have no effect on viral infections. Typically, antibiotics are grouped according to their mechanism of action against specific types of bacteria. The main types of antibiotics are penicillins, tetracyclines, sulfonamides, quinolones, cephalosporins, aminoglycosides and macrolides [30].

The clinical overuse of antibiotics for humans and animals has led to the existence of active pharmaceutical ingredients of antibiotics in the environment, particularly in domestic wastewater (concentrations range from ng L^{-1} to μg L^{-1}) and in hospital and pharmaceutical manufacturing wastewater (concentrations 100–500 mg·L^{-1}) [31]. This occurrence has caused a huge human health problem due to the consequential development of multiresistant bacteria. Therefore, the development of AOPs for antibiotic degradation

in wastewaters is currently a topic of utmost relevance. The structures of the antibiotics degraded by TMP so far are shown in Figure 1.

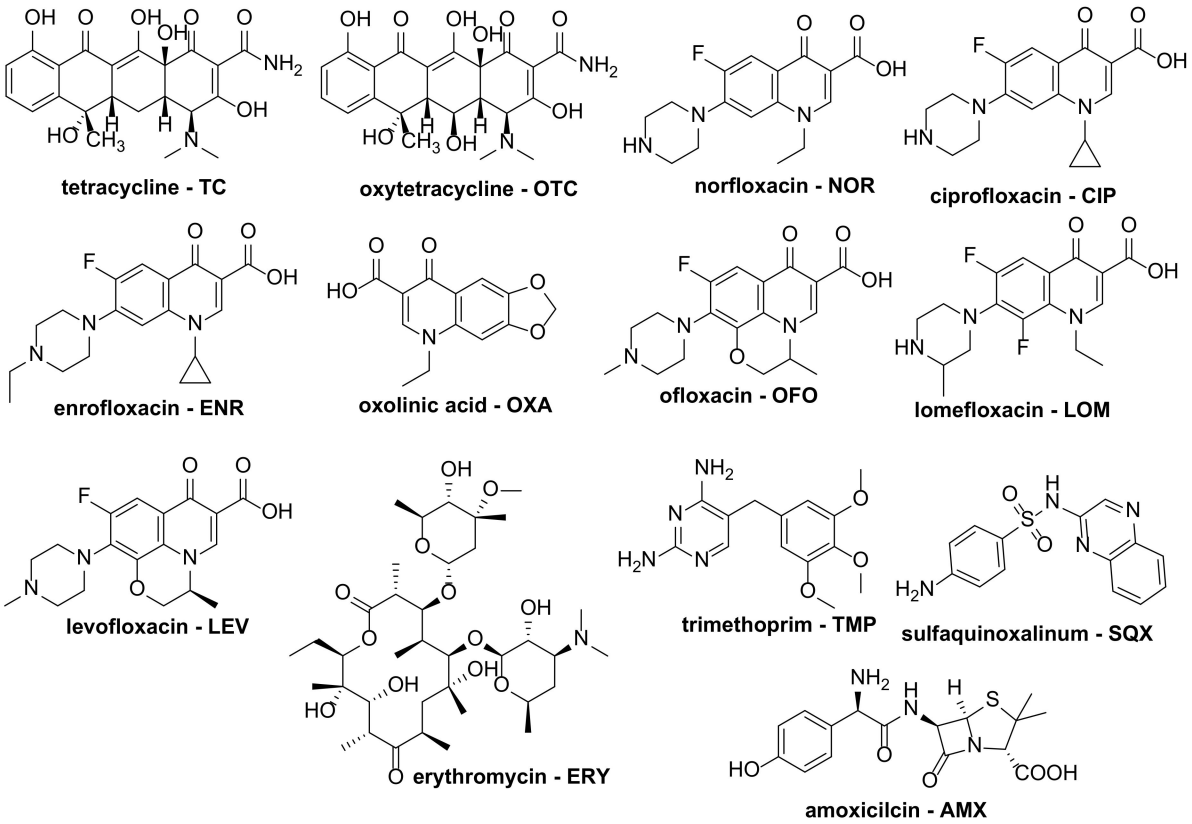

Figure 1. Structures of antibiotics tested in TPM-catalyzed degradation in the last decade.

2.1. Photochemical Degradation

Several TPM-based photocatalysts have been used in the degradation of antibiotics, and their main structures are presented in Figure 2. Antibiotics of the tetracycline family (tetracycline—**TC**, oxytetracycline—**OTC** and their corresponding hydrochloride salts—**TC·HCl** and **OTC·HCl**, (Figure 1) are among the most prescribed and, fortunately, among the most studied regarding their photodegradation (Table 1, entries 1–12).

Several authors incorporated phthalocyanines onto semiconducting photocatalysts, e.g., α-substituted zinc(II) tetra(4-carboxyphenyl)phthalocyanine (**α-ZnTCPc**, Figure 2) embedded onto **g-C_3N_4** (**α-ZnTCPc@g-C_3N_4**) [31], copper(II) β-tetranitrophthalocyanine (**CuTNPc**, Figure 2) deposited on the surface of **CeO_2/Bi_2MoO_6** nanoflowers (**TNCuPc@CeO_2/Bi_2MoO_6**) [21], copper(II) phthalocyanine (**CuPc**, Figure 2) adsorbed onto polyoxometalate nanorods of the type $Ag_xH_{3-x}PMo_{12}O_{40}$ (**CuPc@AgHPMo$_{12}$**) [32] and zinc β-tetraaminophthalocyanine (**ZnTAPc**, Figure 2) covalently linked through amide linkages to a **Cu_2O-TiO_2** blend (**ZnTAPc@Cu_2O-TiO_2**) by modification of the TiO_2 surface at the semiconducting **Cu_2O-TiO_2** layer with maleic anhydride, followed by reaction ZnTAP [33]. Visible-light xenon lamps were used as irradiation sources in these experiments, showing efficiencies above 90% in the degradation of **TC** or **TC·HCl**, except with **CuPc@AgHPMo$_{12}$**, which could only degrade **TC·HCl** in 61% (Table 1, entry 3) [32]. It should be emphasized that the best catalysts showed reusability up to four cycles without significant loss of activity, **TNCuPc@CeO_2/Bi_2MoO_6** being the most efficient catalyst (Table 1, entry 2) [21]. The authors described that after 120 min of irradiation with an 800 W xenon visible light, the TOC removal efficiency was 83% for photocatalyst **TNCuPc@CeO_2/Bi_2MoO_6** nanofibers, which shows the high mineralization ability of

these semiconducting nanofibers as a photocatalyst when compared to **TNCuPc** alone (25.5%) and **CeO_2/Bi_2MoO_6** nanofibers (36.4%) [21].

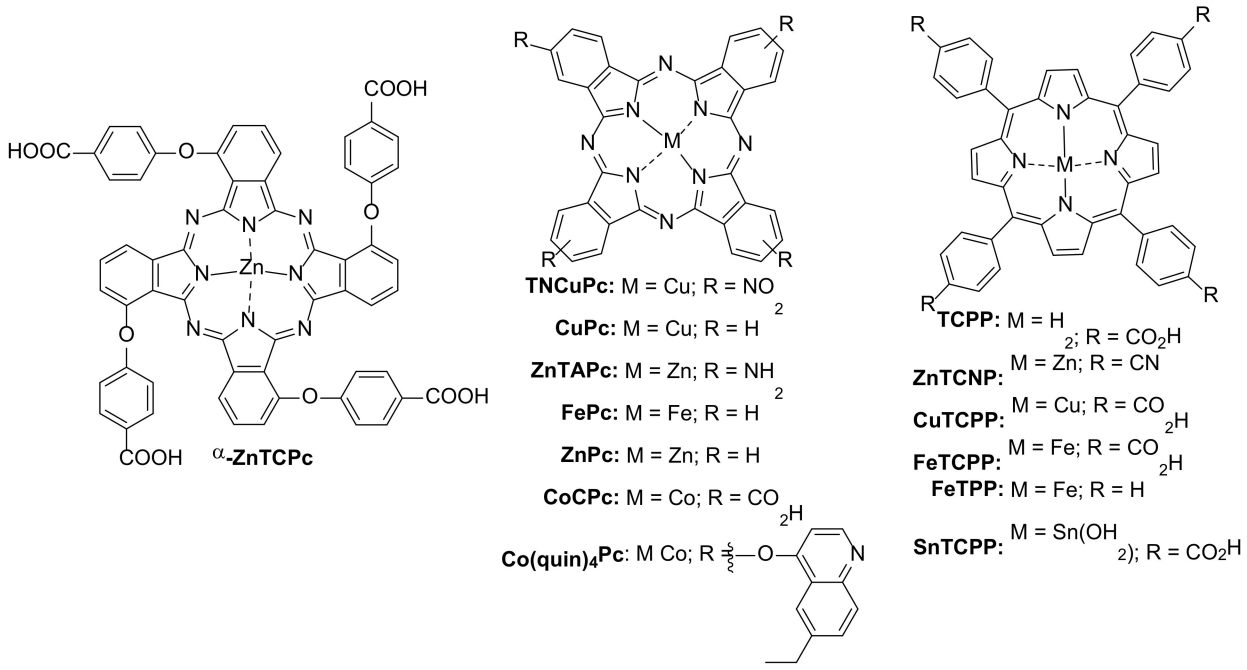

Figure 2. Structures of tetrapyrrolic macrocycles (TPM) used as catalysts for photodegradation of antibiotics.

The authors proposed two pathways for the photodegradation of TC (Scheme 4), HPLC-MS. During the photodegradation process of TC (m/z = 445), some intermediates with the m/z of 402, 360, 318, 290, 274, 242 and 198 were identified, resulting from dechlorination, dihydroxylation, ring-opening reactions and addition-elimination reactions, mainly by $O_2^{\bullet-}$ and HO$^{\bullet}$ ROS species. Prolonged irradiation allowed the formation of small molecular intermediates that were converted to CO_2 and H_2O [21].

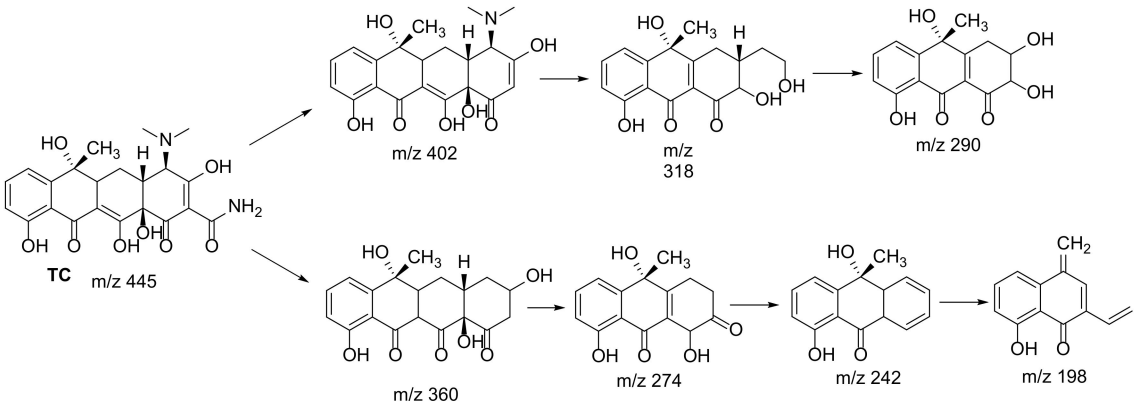

Scheme 4. Proposed pathway for the photodegradation of tetracycline [21].

Similarly, other authors prepared several photocatalysts based on porphyrin derivatives (Table 1, entries 5–7), e.g., *meso*-tetrakis(4-carboxyphenyl)porphyrin (**TCPP**, Figure 2) embedded onto a graphene oxide-Bi_2WO_6, forming the ternary catalyst **TCPP@rGO-Bi_2WO_6** [18], nanostructured zinc(II) *meso*-tetrakis(4-cyanophenyl)porphyrin metal organic complex (**ZnTCNP-MOC**, Figure 2) [34] and copper(II) *meso*-tetra(carboxyphenyl)porphyrin (**CuTCPP**, Figure 2) metal organic framework (**CuTCPP MOF**) [35]. Under visible-light irradiation (visible-light 550 W halogen lamp), the photocatalyst **ZnTCNP-MOC** showed the highest performance, degrading 96% of TC in just 60 min (Table 1, entry 6) [34]. Interest-

ingly, experiments using **CuTCPP MOF** were performed under a low catalyst concentration (0.05 g/L), reaching a satisfactory 72% TC degradation after 6 h of irradiation (Table 1, entry 7) [35]. Only **TCPP@rGO-Bi_2WO_6** was able to be reused in five irradiation cycles (Table 1, entry 5) [18].

Other reports were delivered using tetrapyrrolic macrocycles incorporated onto/into semiconducting blends and used to degrade **TC** antibiotics, e.g., iron(II) *meso*-tetrakis(4-carboxyphenyl) porphyrin (**FeTCPP**, Figure 2) covalently attached to TiO_2 through a toluene diisocyanate (TDI) linker (**FeTCPP@TDI–TiO_2**) [36], iron phthalocyanine (**FePc**, Figure 2) embedded onto semiconductor BiOBr (**FePc@BiOBr**) [37] and *meso* tetra(carboxyphenyl)porphyrin (**TCPP**, Figure 2) embedded onto BiOCl (**TCPP@BiOCl**) [19] (Table 1, entries 8–10). Under visible-light irradiation with a 150 W xenon lamp, Yao and Zhang performed the full degradation of a 25 mg/L solution of **TC·HCl** in 120 min using the hybrid catalyst **FeTCPP@TDI–TiO_2** with a 1 g/L concentration [36], displaying a pseudo-first-order reaction kinetics with $k_{obs} = 2.9 \times 10^{-2}$ min^{-1} (Table 1, entry 8). On the other hand, Xia's group used bismuth oxyhalide as semiconductors instead of titanium dioxide, adsorbing **FePc** and **TCPP** onto **BiOBr** and **BiOCl**, respectively [19,37]. These results showed lower degradation rates (65% and 74% **TC** degradation for **FePc@BiOBr** and **TCPP@BiOCl**, respectively; Table 1, entries 9 and 10), using just 0.4 g/L catalyst loading. Additionally, these catalysts showed high reusability along several cycles. It should be emphasized that some of the above reports also included degradation pathways for TC, proposing the structural assignment of most oxidation products, based on HPLC analysis [21,34,36].

Table 1. Photochemical degradation of antibiotics using TPM-based catalysts.

#/Ref	Catalyst	Drug	Experimental Conditions	Comments
1 [31]	**α-ZnTCPc@g-C_3N_4**	[**TC**] = 30 mg/L	- Matrix: Distilled water - Visible-light xenon lamp λ > 400 nm (power: N/A) - [**α-ZnTCPc@g-C_3N_4**] = 1 g/L - pH = N/A; T = N/A - Pre-dark for 30 min	- 91% **TC** in 120 min - TOC: N/A - k_{obs}: N/A - Mechanism by $HO^{\bullet}$ - Reutilization: 5 cycles
2 [21]	**TNCuPc@CeO_2/Bi_2MoO_6**	[**TC**] = 50 mg/L	- Matrix: Distilled water - Visible-light 800 W xenon lamp λ > 400 nm - -[**TNCuPc@CeO_2/Bi_2MoO_6**] = 1.5 g/L - pH = N/A; T = N/A - Pre-dark for 30 min	- 95% **TC** in 120 min - 84% TOC decrease in 120 min - k_{obs}: N/A - Mechanism by h^+, $O_2^{\bullet-}$ - Degradation pathway proposed - Reutilization: 4 cycles
3 [32]	**CuPc@$AgHPMo_{12}$**	[**TC·HCl**] = 20 mg/L	- Matrix: Distilled water - Visible-light 500 W xenon lamp λ > 400 nm - [**CuPc@$AgHPMo_{12}$**] = 1 g/L - pH = N/A; T = N/A	- 61% **TC·HCl** in 180 min - TOC: N/A - k_{obs}: N/A - Mechanism by h^+ - Reutilization: N/A
4 [33]	**ZnTAPc@Cu_2O-TiO_2**	[**TC·HCl**] = 20 mg/L	- Matrix: Distilled water - Visible-light 300 W xenon lamp λ > 420 nm - [**ZnTAPc@Cu_2O-TiO_2**] = 0.5 g/L - pH = 6; T = 25 °C	- 95% **TC·HCl** in 200 min - TOC: N/A - k_{obs}: N/A - Mechanism by h^+, $O_2^{\bullet-}$ - Reutilization: 4 cycles
5 [18]	**TCPP@rGO-Bi_2WO_6**	[**TC**] = 15 mg/L	- Matrix: Distilled water - Visible-light 300 W xenon lamp λ > 420 nm - [**TCPP@rGO-Bi_2WO_6**] = 0.3 g/L - pH = 7.3; T = N/A - Pre-dark for 30 min	- 84% **TC** in 60 min - TOC: N/A - k_{obs}: N/A - Mechanism by $O_2^{\bullet-}$, h^+ - Reutilization: 5 cycles

Table 1. *Cont.*

#/Ref	Catalyst	Drug	Experimental Conditions	Comments
6 [34]	**ZnTCNP MOC**	**[TC]** = 5 mg/L	- Matrix: Distilled water - Visible-light 550 W halogen lamp λ > 420 nm - **[ZnTCNP MOC]** = 1 g/L - pH = 7.3; T = N/A - Pre-dark for 20 min	- 96% **TC** in 60 min - TOC: N/A - k_{obs}: N/A - Mechanism by $HO^{\bullet}$, $O_2^{\bullet-}$ - Degradation pathway proposed - Reutilization: N/A
7 [35]	**CuTCPP MOF**	**[TC]** = 40 mg/L **[NOR]** = 20 mg/L	- Matrix: Distilled water - Visible-light 300 W xenon lamp λ > 420 nm - **[CuTCPP MOF]** = 0.05 g/L - pH = 5–9; T = 25 °C - Pre-dark: N/A	- 72% **TC** (pH = 5), 44% **NOR** (pH = 9) degradation in 360 min - TOC: N/A - 2nd order k_{obs}: dominated by adsorption - Mechanism by h^+ and $O_2^{\bullet-}$ - Reutilization: N/A
8 [36]	**FeTCPP@TDI–TiO_2**	**[TC·HCl]** = 25 mg/L **[NOR]** = 25 mg/L	- Matrix: Distilled water - Visible-light 150 W xenon lamp λ > 400 nm - **[FeTCPP@TDI–TiO_2]** = 1 g/L - pH = N/A; T = N/A - Pre-dark for 30 min	- >99% **TC·HCl** and **NOR** degradation in 120 min - TOC: N/A - k_{obs} (**TC**) = 2.9×10^{-2} min^{-1} - k_{obs} (**NOR**) = 3.4×10^{-2} min^{-1} - Mechanism: N/A - Degradation pathway proposed - Reutilization: 5 cycles (**TC**)
9 [37]	**FePc@BiOBr**	**[TC]** = 20 mg/L **[CIP]** = 10 mg/L	- Matrix: Distilled water - Visible-light 350 W xenon lamp λ > 400 nm - **[FePc@BiOBr]** = 0.4 g/L - pH = N/A; T = N/A - Pre-dark for 1 h	- ~65% **TC** and ~55% **CIP** degradation in 240 min - TOC: N/A - k_{obs}: N/A - Mechanism by h^+, $HO^{\bullet}$, $O_2^{\bullet-}$ - Reutilization: 3 cycles
10 [19]	**TCPP@BiOCl**	**[TC]** = 20 mg/L **[CIP]** = 10 mg/L **[ENR]** = 10 mg/L	- Matrix: Distilled water - Visible-light 250 W xenon lamp λ > 400 nm - **[TCPP@BiOCl]** = 0.4 g/L - pH = N/A; T = 30 °C - Pre-dark for 30 min	- 74% **TC**, 42% **CIP** and 60% **ENR** degradation in 120 min - TOC: N/A - k_{obs}: 1.1×10^{-2} min^{-1} (**TC**) - Mechanism by $HO^{\bullet}$, h^+, $O_2^{\bullet-}$ - Reutilization: 4 cycles (**TC**)
11 [38]	**FePc@N-PR**	**[OTC·HCl]** = 100 mg/L	- Matrix: Distilled water - Visible-light 50 W halogen lamp λ > 420 nm - **[FePc@N-PR]** = 0.75 g/L - $[H_2O_2]$ = 60 mM - pH = 5.3; T = 35 °C	- 94% **OTC·HCl** degradation in 500 min - TOC: N/A - k_{obs}: N/A - Mechanism by $HO^{\bullet}$ - Reutilization: 5 cycles
12 [17]	**MTCPP@TiO_2**M = H_2, Zn and Cu	**[OTC]** = ~8 mg/L **[OXA]** = ~8 mg/L	- Matrix: Distilled water - Sunlight simulator 300 W - **[MTCPP@TiO_2]** = 0.02 g/L - Irradiation time: 40 min - pH = 7; T = N/A - Pre-dark for 15 min	- 63% **OTC**, 68% **OXA** degradation in 40 min (with **CuTCPP@TiO_2** - TOC: N/A - k_{obs}: N/A - Mechanism: N/A - Reutilization: N/A
13 [39]	**FeTPP@Cr-TiO_2**	**[NOR]** = 25 mg/L **[OFO]** = 25 mg/L **[LOM]** = 25 mg/L	- Matrix: Distilled water - Visible-light 150 W xenon lamp λ > 400 nm - **[FeTPP@Cr-TiO_2]** = 1 g/L - pH = N/A; T = N/A - Pre-dark for 30 min	- 98% **NOR**, 99% **OFO**, ~100% **LOM** degradation in 120 min - TOC: N/A - k_{obs} (**NOR**) = 2.8×10^{-2} min^{-1} - k_{obs} (**OFO**) = 3.9×10^{-2} min^{-1} - k_{obs} (**LOM**) = 3.0×10^{-2} min^{-1} - Mechanism: N/A - Reutilization: N/A

Table 1. *Cont.*

#/Ref	Catalyst	Drug	Experimental Conditions	Comments
14 [40]	**PCN-222@g-C_3N_4(PCN-222 = FeTCPP Zr-MOF)**	[**OFO**] = 20 mg/L	- Matrix: Distilled water - Visible-light 300 W xenon lamp > 400 nm - [**PCN-222@g-C_3N_4**] = 1 g/L - pH = N/A; T = N/A - Pre-dark for 120 min	- 96% **OFO** in 200 min - 89% TOC decrease in 12 h - k_{obs}: 1.4 × 10^{-2} min^{-1} 1. Mechanism by h^+, $HO^•$, $O_2^{•-}$ - Reutilization: 4 cycles
15 [41]	**PCN-222@PW_{12}/TiO_2(PCN-222 =FeTCPP Zr-MOF)**	[**OFO**] = 20 mg/L	- Matrix: Distilled water - Visible-light 300 W xenon lamp > 400 nm - [**PCN-222@PW_{12}/TiO_2**] = 0.4 g/L - pH = N/A; T = N/A - Pre-dark for 2 h	- 95% **OFO** in 120 min - 91% TOC decrease in 10 h - k_{obs}: 2.2 × 10^{-2} min^{-1} - Mechanism by h^+, $HO^•$, $O_2^{•-}$ - Reutilization: 4 cycles
16 [42]	**SnTCPP@g-C_3N_4/Bi_2WO_6**	[**LEV**] = 10 mg/L	- Matrix: Distilled water - Visible-light 250 W xenon lamp λ > 400 nm - [**SnTCPP@g-C_3N_4/Bi_2WO_6**] = 1 g/L - pH = 7.3; T = N/A - Pre-dark for 30 min	- 86% LEV in 150 min - 59% TOC decrease in 4 h - k_{obs}: N/A - Mechanism by $HO^•$ - Degradation pathway proposed - Reutilization: N/A
17 [43]	**ZnPc@TiO_2**	[**ERY**] = 7.5 mg/L	- Matrix: Distilled water - Visible-light 300 W xenon lamp λ > 400 nm - [**ZnPc@TiO_2**] = 0.4 g/L - Pre-dark for 30 min - pH = 5; T = 20 °C	- 74% **ERY** degradation in 180 min - TOC: N/A - k_{obs}: N/A - Mechanism: N/A - Reutilization: 5 cycles
18 [44]	**FePc@P4VP/PET**	[**SQX**] = 6 mg/L	- Matrix: Distilled water - UV-light 150 W mercury lamp - [**FePc@P4VP/PET**] = 2 g/L - [H_2O_2] = 10 mM - pH = 7; T = 50 °C	- 95% **SQX** in 240 min - TOC: N/A - k_{obs}: N/A - Mechanism by $HO^•$, $HOO^•$, and Fe(IV) = O - Reutilization: 5 cycles
19 [16]	**CoCPc@K-TiO_2**	[**TMP**] = 25 mg/L	- Matrix: Distilled water - UV-light 150 W mercury lamp - [**CoCPc@K-TiO_2**] = 0.75 g/L - pH = N/A; T = 25–45 °C	- 54% **TMP** in 240 min - TOC: N/A - k_{obs}: N/A - Mechanism by $HO^•$ - Degradation pathway proposed - Reutilization: 5 cycles
20 [45]	**Co(quin)$_4$Pc@TiO_2**	[**AMX**] = 20 mg/L	- Matrix: Distilled water - UV-light 12 W lamp - [**Co(quin)$_4$Pc@TiO_2**] = 1 g/L - pH = N/A; T = 25 °C	- 41% **AMX** in 150 min - TOC: N/A - k_{obs}: N/A - Mechanism by $HO^•$ - Reutilization: N/A

Sun-prepared **FePc@N-PR**, by covalent grafting of iron phthalocyanine (**FePc**, Figure 2) onto a macroporous chloromethylated polystyrenedivinylbenzene resin (**PR**), partially pre-functionalized with 4-aminopyridine [38]. This ligand (denoted as **N**) was then used as an axial ligand to further coordinate the iron complex inside the resin. This catalyst (concentration = 0.75 g/L) was used to promote the photodegradation of oxytetracycline hydrochloride (**OTC·HCl**, Figure 2), using hydrogen peroxide (60 mM) as oxidant. A 94% degradation was observed in 500 min, and the catalyst was capable of being reused along 5 cycles without significant degradation [38] (Table 1, entry 11).

D'Urso prepared **MTCPP@TiO_2** catalysts by adsorption of **MTCPP** (where M = H_2, Zn or Cu) (Figure 2) onto **TiO_2** [17]. These catalysts (concentration = 0.02 g/L) were evaluated in the degradation of oxytetracycline (**OTC**, Figure 2), and similar results were obtained. The best catalyst, **CuTCPP@TiO_2**, gave 63% **OTC** photodegradation in 40 min of irradiation with a 300 W sunlight simulator (Table 1, entry 12).

Besides tetracyclines, other antibiotics have also been photodegraded, e.g., the quinolone family (Figure 1). Under visible-light irradiation (300 W Xe lamp), Li used **CuTCPP MOF** as a photocatalyst (concentration = 0.05 g/L) to promote the degradation of norfloxacin (**NOR**, Figure 1), reaching 44% degradation after 6 h of irradiation (Table 1, entry 7) [35]. Additionally, Yao used **FeTCPP@TDI–TiO_2** as a catalyst (concentration = 1 g/L) to degrade the same antibiotic, reaching full degradation in just 2 h irradiation (Table 1, entry 8). This result emphasizes the influence of the toluene diisocyanate (TDI) linker, which allowed a higher efficiency, when compared with **FeTCPP** directly adsorbed onto **TiO_2** or **TDI-TiO_2** [36].

Xia used **FePc@BiOBr** and **TCPP@BiOCl** (concentration = 0.4 g/L) as photocatalysts in the degradation of ciprofloxacin (**CIP**, Figure 1). These catalysts were able to degrade **CIP** in 55% and 42%, respectively, after 4 h and 2 h of visible-light Xe-lamp irradiation, respectively (Table 1, entries 9 and 10) [19,37]. **TCPP@BiOCl** was further used as a photocatalyst to degrade enrofloxacin (**ENR**, Figure 1), reaching 60% degradation after 120 min of irradiation (Table 1, entry 10) [19]. Additionally, the same group prepared the catalyst **FeTPP@Cr-TiO_2** by adsorbing **FeTPP** (Figure 2) onto chromium-doped **TiO_2** [39]. With a catalyst concentration of 1 g/L, **NOR** was 98% degraded after 2 h of irradiation with 150 W Xe-lamp visible light, (Table 1, entry 13). This catalyst induced a first-order reaction-rate kinetics, with $k_{obs} = 2.8 \times 10^{-2}$ min^{-1}, while **FeTCPP@TDI–TiO_2**, reported by the same group, displayed $k_{obs} = 3.4 \times 10^{-2}$ min^{-1} (Table 1, entry 8) [36].

Another recurrently tested antibiotic is ofloxacin (**OFO**, Figure 1). In that respect, Xu's group reported the synthesis of **PCN-222@g-C_3N_4** [40] and **PCN-222@PW_{12}/TiO_2** [41] catalysts, where **PCN-222** is a zirconium-based MOF capable of incorporating **FeTCPP** (Figure 2) units (Figure 3) [46].

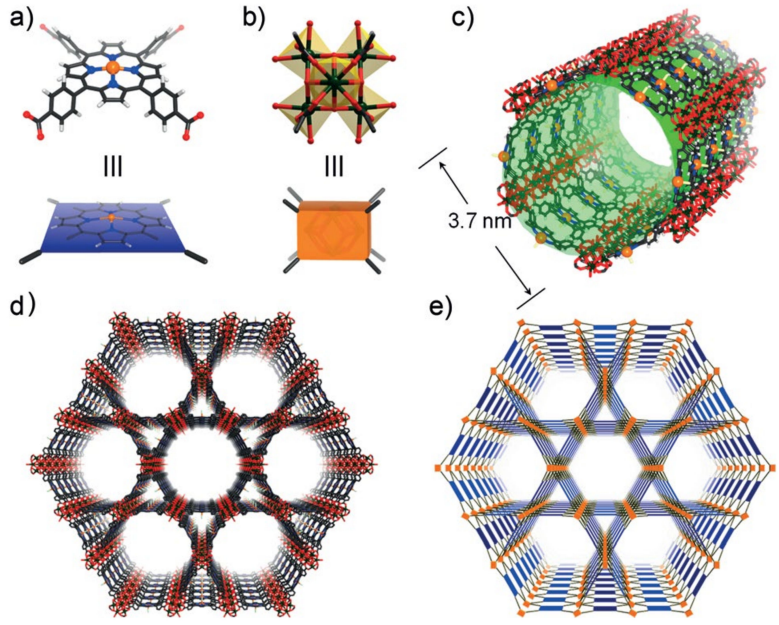

Figure 3. Crystal structure and underlying network topology of PCN-222(Fe). The **Fe-TCPP** ((**a**); blue square) is connected to four 8-connected Zr6 clusters ((**b**); light orange cuboid) with a twisted angle to generate a 3D network in Kagome-like topology (**d**,**e**) with 1D large channels ((**c**); green pillar). Zr black spheres, C gray, O red, N blue, Fe orange. H atoms were omitted for clarity. Adapted with permission from ref. [46]. Copyright 2012 John Wiley & Sons.

First, the MOF was adsorbed onto **g-C_3N_4** and **PW_{12}/TiO_2** blends, respectively. The catalysts, along with **FeTPP@Cr-TiO_2** [39], were tested in the degradation of **OFO** under 150 W Xe-lamp visible-light irradiation, and the latter was slightly more efficient, with 99% degradation in 120 min (Table 1, entry 13), when compared to 96% (200 min) and 95% (120 min) for **PCN-222@g-C_3N_4** and **PCN-222@PW_{12}/TiO_2**, respectively (Table 1, entries 14 and 15). The first-order reaction kinetics were measured, and k_{obs} followed the order **FeTPP@Cr-TiO_2** > **PCN-222@PW_{12}/TiO_2** > **PCN-222@g-C_3N_4** (k_{obs} = 3.9 × 10^{-2} min^{-1}, 2.2 × 10^{-2} min^{-1} and 1.4 × 10^{-2} min^{-1}, respectively). Interestingly, **PCN-222@g-C_3N_4** and **PCN-222@PW_{12}/TiO_2**-based MOF catalysts were able to reach a TOC decrease of 89% (12 h) and 91% (10 h), respectively, and could be reused up to four cycles successfully [40,41].

D'Urso used the **MTCPP@TiO_2** catalysts (M = H_2, Zn and Cu) to degrade oxolinic acid (**OXA**, Figure 1) under sunlight-simulator irradiation (300 W) and observed that **CuTCPP@TiO_2** was the most active catalyst, with 68% **OXA** degradation in 40 min (Table 1, entry 12) [17]. Yao further studied the degradation of lomefloxacin (**LOM**, Figure 1) using **FeTPP@Cr-TiO_2** as catalyst, reaching complete degradation after 120 min of visible-light irradiation (Table 1, entry 13).

He and Ma prepared an **SnTCPP@g-C_3N_4/Bi_2WO_6** catalyst by adsorbing tin(IV) *meso*-tetrakis(4-carboxyphenyl)porphyrin (**SnTCPP**, Figure 2) onto a semiconducting **g-C_3N_4/Bi_2WO_6** blend [42]. Under visible-light irradiation (250 W Xe lamp), the authors promoted the photodegradation of levofloxacin (**LEV**, Figure 1) at a catalyst concentration of 1 g/L, reaching 86% degradation in 150 min. Furthermore, total organic carbon was measured, and a value of 59% TOC, upon 4 h of irradiation, was described (Table 1, entry 16).

Two decomposition pathways were proposed by the authors (Scheme 5). In pathway I, LEV (*m*/*z* 361) was decarboxylated, providing an intermediate with *m*/*z* 317. Then, via defluorination, demethylation and dehydrogenation on the piperazine ring, the intermediate with *m*/*z* 283 was formed and further demethylated and oxidized to give an intermediate with *m*/*z* 274. Due to the high oxidizing capability of HO•, the piperazine and morpholine ring-opening reactions occurred and the intermediate with *m*/*z* 184 was observed as well. In pathway II, a defluorination LEV anion was found at *m*/*z* 342, which suffered dehydrogenation to produce an intermediate with *m*/*z* 340. Then, the piperazine ring-opening reaction occurred, yielding an intermediate with *m*/*z* 317. Further HO• attack caused the demethylation, deamination, deethylation and decarboxylation reactions to form intermediates with *m*/*z* 246 or *m*/*z* 218, respectively. Finally, those ring-opening intermediates could be further degraded into the other compounds with lower molecular weight, such as CO_2 and H_2O [42].

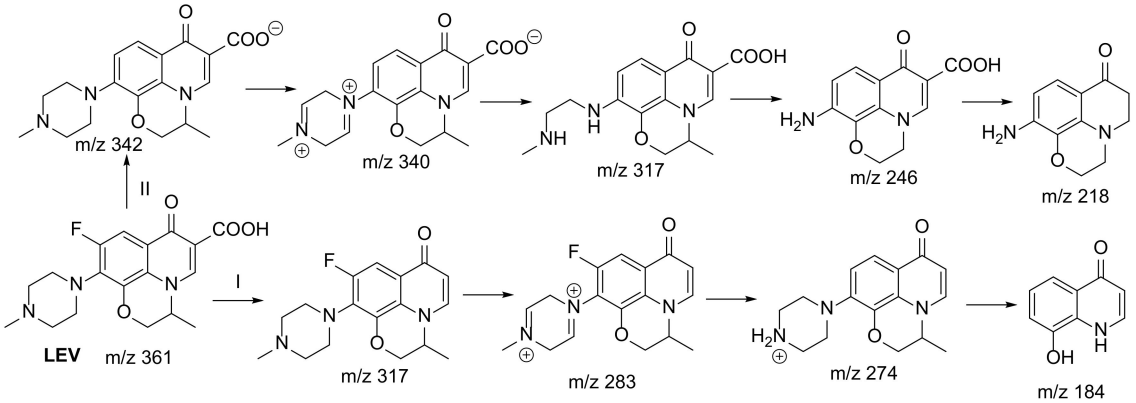

Scheme 5. Proposed pathway for the photodegradation of levofloxacin [42].

Vignesh and Suganthi [43] used zinc phthalocyanine- (**ZnPc**, Figure 2) modified titania nanoparticles (**ZnPc@TiO_2**), prepared by adsorption, to catalyze the photodegradation of erythromycin (**ERY**, Figure 1), obtaining 74% degradation in 180 min under visible-light

irradiation (300 W Xe lamp). The catalyst was used in a 0.4 g/L concentration and could be reused up to five times without significant loss of activity (Table 1, entry 17).

Sulfaquinoxalinum degradation (**SQX**, Figure 1) was also tested. Lu and Chen [44] prepared the hybrid catalyst **FePc@P4VP/PAET** by adsorbing iron phthalocyanine (**FePc**, Figure 2) onto poly(4-vinylpyridine)/polyester (**P4VP/PET**) nanofibers. With a catalyst concentration of 2 g/L, SQX was degraded 95% under ultraviolet light (150 W mercury lamp) after 240 min (Table 1, entry 18). Ciuffi [16] developed a composite photocatalyst, by mixing, under sol-gel conditions, kaolinite, TiO_2 and cobalt(II) tetracarboxyphthalocyanine (**CoCPc**, Figure 2), obtaining a **CoCPc@K-TiO$_2$** hybrid catalyst. The authors promoted the degradation of trimethoprim (**TMP**, Figure 1) under ultraviolet irradiation (150 W mercury lamp) using a catalyst concentration of 0.75 g/L. Under those conditions, the authors described a 54% degradation of TMP in 240 min, and the catalyst was reused without significant loss of activity for up to five cycles (Table 1, entry 19).

Sökmen [45] reported the synthesis of **Co(quin)$_4$Pc@TiO$_2$** by impregnation of **Co(quin)$_4$Pc** (Figure 2) onto semiconducting TiO_2. The catalyst, in a concentration of 1 g/L, was used in the photodegradation of amoxicilin (**AMX**, Figure 1), and 40% degradation was obtained after 150 min using a UV light lamp (12 W) at 254 nm. Nevertheless, neat TiO_2 induced 38% degradation under the same conditions, which can be ascribed to the use of the UV light source, which enables TiO_2 photocatalytic properties (Table 1, entry 20).

2.2. Oxidative Chemical Degradation

Martins [47–49] used a set of *meso*-tetrasubstituted porphyrins as catalysts for the degradation of antibiotics **CIP**, **LEV** and **NOR** (Figure 1). Chloro *meso*-tetraphenylporphyrinato manganese(III) (**Mn^{III}(TPP)Cl**, Figure 4), chloro *meso*-tetrakis(4-carboxyphenyl)porphyrinato manganese(III) (**Mn^{III}(TCPP)Cl**, Figure 4), chloro *meso*-β-octabromo-tetrakis(4-carboxyphenyl) porphyrinato manganese(III) (**Mn^{III}(Br$_8$TCPP)Cl**, Figure 4), chloro *meso*-tetrakis(2,3-dichlorophenyl) porphyrinato manganese(III) (**Mn^{III}(T2,3DCPP)Cl**, Figure 4) and chloro *meso*-tetrakis(2-fluoro-6-chlorophenyl)porphyrinato manganese(III), (**Mn^{III}(T2,6CFPP)Cl**, Figure 4) were chosen as catalysts and water/acetonitrile mixture was chosen as a solvent under homogeneous conditions (Table 2, entries 1–3). In the first study, the authors used **Mn^{III}(TCPP)Cl**, and several oxidants were evaluated, such as iodosobenzene, hydrogen peroxide and *meta*-chloroperoxybenzoic acid (mCPBA). Among them the best oxidant to promote full **CIP** degradation (100%) was the toxic iodosobenzene (PhIO) (Table 2, entry 1) [47]. Further studies were performed using diacetoxyiodobenzene ($PhI(OAc)_2$), but no improvements were observed (Table 2, entry 2) [48]. Further studies on **NOR** degradation, using **Mn^{III}(T2,3DCPP)Cl** and **Mn^{III}(T2,6CFPP)Cl** as catalysts, revealed that these catalysts were similarly active, reaching 58% and 57% **NOR** degradation, respectively, using PMS as the oxidant (Table 2, entry 3) [49].

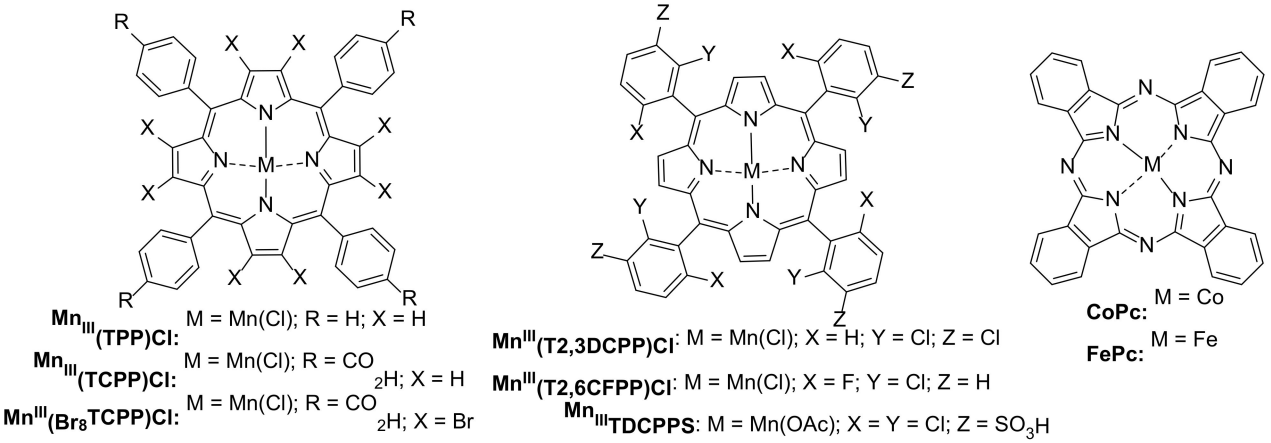

Figure 4. Structures of tetrapyrrolic macrocycles (TPM) used as catalysts for oxidative chemical degradation of antibiotics.

Table 2. Oxidative degradation of antibiotics using TPM-based catalysts.

#/Ref	Catalyst	Drug	Experimental Conditions	Comments
1 [47]	**Mn^{III}(TPP)Cl**, **Mn^{III}(TCPP)Cl**, **Mn^{III}(Br_8TCPP)Cl**	[**CIP**] = 10 mg/L	- Homogeneous - Matrix: Distilled water/acetonitrile - [**Mn^{III}(TPP)Cl**] = 0.02 g/L; [**Mn^{III}(TCPP)Cl**] = 0.03 g/L; [**Mn^{III}(Br_8TCPP)Cl**] = 0.04 g/L - [oxidant] = 3×10^{-4} M (PhIO, H_2O_2, MCPBA) - pH = N/A; T = 25 °C	- 100% **CIP** degradation in 24 h (with **Mn^{III}(TCPP)Cl** and PhIO) - TOC decrease: N/A - k_{obs}: N/A - Mechanism by $HO^{\bullet}$ - Degradation pathway proposed - Reutilization: N/A - Cytotoxicity studies on human embryonic kidney cells HEK-293 (no toxicity found, both for CIP and oxidation products)
2 [48,50]	**Mn^{III}(TCPP)Cl**, **Mn^{III}(Br_8TCPP)Cl**	[**CIP**] = 10 mg/L [**LEV**] = 10 mg/L [**NOR**] = 10 mg/L	- Homogeneous - Matrix: Distilled water/acetonitrile - [**Mn^{III}(TCPP)Cl**] = 0.03 g/L; [**Mn^{III}(Br_8TCPP)Cl**] = 0.04 g/L - -[oxidant] = 3×10^{-4} M - (PhIO, PhI($OAc)_2$, H_2O_2, MCPBA) - pH = N/A; T = 25 °C	- 100% **CIP** degradation in 24 h (with **Mn^{III}(TCPP)Cl** and PhIO) - 98% **LEV** degradation in 24 h [with **Mn^{III}(TCPP)Cl** and PhI(OAc_2)] - TOC decrease: N/A - k_{obs}: N/A - Mechanism by $HO^{\bullet}$ - Degradation pathway proposed for **LEV** - Reutilization: N/A
3 [49]	**Mn^{III}(TPP)Cl**, **Mn^{III}(T2,3DCPP)Cl**, **Mn^{III}(T2,6CFPP)Cl**	[**NOR**] = 14 mg/L (stock)	- Homogeneous - Matrix: Distilled water/acetonitrile - [**Mn^{III}(T2,3DCPP)Cl**] = 0.04 g/L; [**Mn^{III}(T2,6CFPP)Cl**] = 0.04 g/L - [oxidant] = 2×10^{-6} M - (H_2O_2, ^{t}BuOOH, PMS) - pH < 6; T = 25 °C	- 58% **NOR** degradation by **Mn^{III}(T2,3DCPP)Cl**, 57% **NOR** degradation by **Mn^{III}(T2,6CFPP)Cl** in 24 h (with PMS) - TOC decrease: N/A - k_{obs}: N/A - Mechanism by $HO^{\bullet}$, $SO_4^{\bullet-}$ - Degradation pathway proposed - Reutilization: N/A - Cytotoxicity studies human peripheral blood mononuclear cells (no toxicity found, both for **NOR** and oxidation products)
4 [51]	**CoPc@GO**	[**NOR**] = 10 mg/L	- Matrix: Distilled water - [**CoPc@GO**] = 0.1 g/L - [PMS] = 6.5×10^{-3} M - pH = 7; T = N/A	- 100% **NOR** degradation in 60 min - TOC: N/A - k_{obs}: N/A - Mechanism by $HO^{\bullet}$, $SO_4^{\bullet-}$ - Reutilization for 3 cycles
5 [52]	**FePc@N-PR**	[**TC·HCl**] = 100 mg/L	- Matrix: distilled water, tap water, wastewater - [R-N-Fe] = 1.0 g/L - [PMS] = 2.0 mM - pH = 6; T = 45 °C	- 83% **TC·HCl** degradation in 280 min - 30% TOC decrease in 280 min - k_{obs}: N/A - Mechanism by $HO^{\bullet}$, $SO_4^{\bullet-}$ - Degradation pathway proposed - Reutilization: 5 cycles
6 [53]	**FePc@P4VP/PAN**	[**SQX**] = 6 mg/L	- Matrix: Distilled water, wastewater - [**FePc@P4VP/PAN**] = 1.0 g/L - [H_2O_2] = 10 mM - pH = 3; T = 50 °C	- 95% **SQX** degradation in 120 min - TOC decrease: N/A - k_{obs}: N/A - Mechanism by $HO^{\bullet}$ - Degradation pathway proposed - Reutilization: N/A
7 [54]	**MnTDCPPS@N-SiO_2**	[**TMP**] = 130 mg/L	- Matrix: Distilled water - [**MnTDCPPS@N-SiO_2**] = 0.002 g/L - [H_2O_2] = 0.26 mM - pH = 7; T = 25 °C	- 95% TMP degradation in 150 min - 24% TOC decrease in 150 min - k_{obs}: = 2.0×10^{-2} min^{-1} - Mechanism by $HO^{\bullet}$ - Degradation pathway proposed - Reutilization: 5 cycles - -ecotoxicity studies on *V. fischeri*, *R. subcapitata* and *B. calyciflorus* (oxidation products slightly increase toxicity)

Zhang [51] prepared the hybrid catalyst **CoPc@GO** by adsorption of cobalt phthalocyanine (**CoPc**, Figure 4) onto graphene oxide (**GO**). **NOR** was 100% degraded in 60 min using a catalyst concentration of 0.1 g/L and 6.5 × 10^{-3} M PMS (as oxidant) (Table 2, entry 4). Sun [52] used the hybrid catalyst **FePc@N-PR**, having iron phthalocyanine (**FePc**, Figure 2) units covalently attached to macroporous chloromethylated polystyrenedivinylbenzene resin (**PR**) [38] and used it to promote the degradation of **TC·HCl**, with PMS as oxidant, at pH = 6 and a temperature of 45 °C. With a catalyst concentration of 1 g/L, in the presence of a PMS solution (2.0 mM), 83% **TC·HCl** degradation was achieved in 280 min, with a TOC decrease of 30% (Table 2, entry 5). The authors further tested different matrices, in addition to distilled water, and found that in tap water, the degradation was accelerated, probably due to the presence of Cl^- or HCO_3^-, which may react with PMS and generate further reactive chlorine species. On the other hand, the same experiment in wastewater was inhibited, probably due to the presence of organic impurities that can block the catalyst's activity [52].

Lu and Chen [53] prepared hybrid catalysts **FePc@P4VP/PAN** by adsorbing iron phthalocyanine (**FePc**, Figure 4) onto poly(4-vinylpyridine)/polyacrylonitrile (**P4VP/PAN**) nanofibers. Using a catalyst concentration of 1 g/L, in the presence of a 10 mM H_2O_2 solution (as oxidant), 95% of **SQX** was degraded in 120 min at pH = 3 and a temperature of 50 °C.

Pereira and Calvete [54] reported the synthesis of an **MnTDCPPS@N-SiO$_2$** hybrid catalyst by covalent attachment of acetate *meso*-tetrakis(2,6-dichloro-3-sulfophenyl)porphyrinato manganese(III) (**MnTDCPPS**, Figure 4) to aminopropylsilyl-functionalized silica (**N-SiO$_2$**). Remarkably, the immobilized catalyst, despite being used in quite a low concentration (0.002 g/L) and in the presence of 0.26 mM H_2O_2 as oxidant, was able to promote the oxidative degradation of trimethoprim (**TMP**, Figure 1) in 95% (24% TOC decrease) after 150 min at pH = 7 and 25 °C. The catalyst could be reused up to five cycles without losing its activity (Table 2, entry 7).

The authors proposed a degradation pathway for TMP (Scheme 6) and observed that the major processes involved in the degradation of TMP were hydroxylation, oxidation and demethylation, mostly by $HO^{\bullet}$. TMP could fully (m/z 248) or partially (m/z 291) demethylate, besides undergoing hydroxylation (m/z 307). This intermediate could further undergo hydroxylation, giving m/z 323, or oxidize into m/z 305. This last intermediate could either demethylate to give m/z 291 or hydroxylate to provide m/z 321. This intermediate could also be produced by oxidation of m/z 323 by direct oxidation. Ultimately, the m/z 291 intermediate could further suffer cleavage to yield m/z 187 [54].

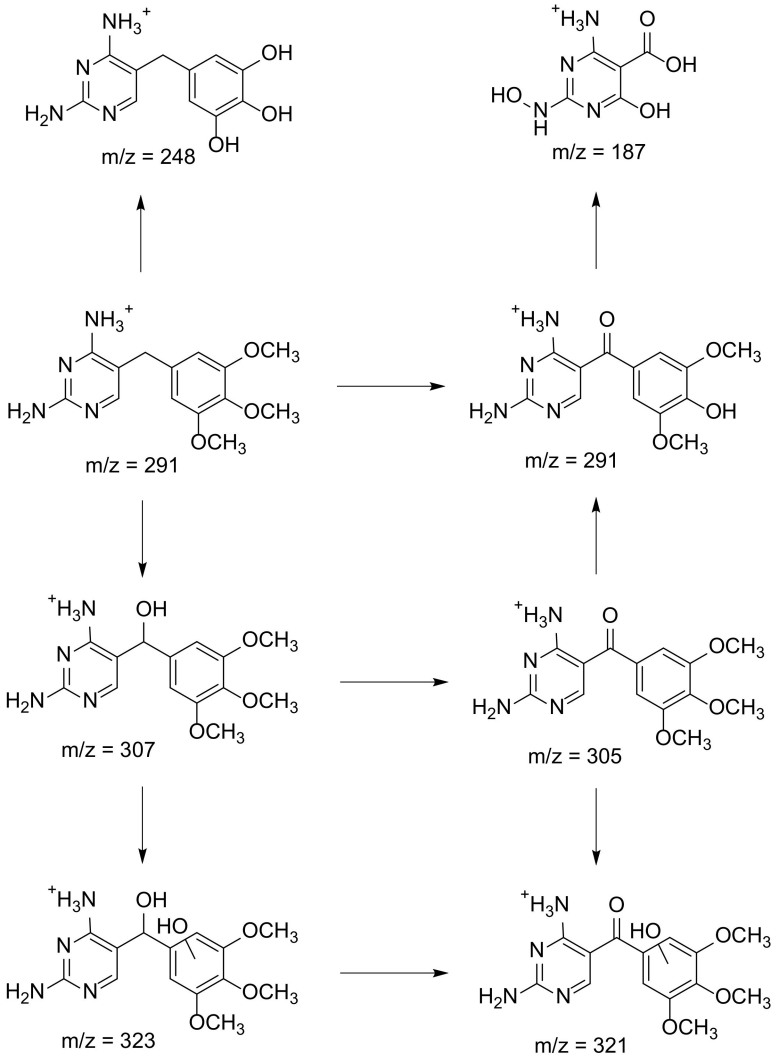

Scheme 6. Proposed pathway for degradation of trimethoprim [54].

3. Degradation of Analgesic Drugs

Analgesics are drugs that relieve different types of pain. Most prescribed analgesics include anti-inflammatory drugs, which reduce inflammation (e.g., ibuprofen, diclofenac, acetaminophen derivatives and salicylic acid, known as nonsteroidal anti-inflammatory drugs), and opioid analgesics, which change the way the brain perceives pain (e.g., tramadol). These types of drugs are commonly encountered in municipal wastewaters since they are consumed in quite high quantities by the general population [55,56].

Dabrowski's group investigated the photocatalytic degradation of tramadol (**TRML**, Figure 5) (Table 3, entry 1) [57] using LED-light irradiation (λ = 530 nm with light doses from 1 to 20 J cm^{-2}). The authors were able to degrade 80% of **TRML** in 60 min, using **ZnTDFPPS@TiO$_2$** as hybrid catalyst (Figure 6). The zinc(II) *meso*-tetra-(2,6-difluoro-3(5)-sulfonatophenyl)porphyrin (**ZnTDFPPS**) was incorporated by impregnation (concentration = 0.67 g/L). Additionally, the authors did not observe any photocatalytic activity when **TiO$_2$** was used under the same reaction conditions. The best results obtained with the hybrid catalyst were attributed to its higher visible-light absorption, with subsequent higher formation of ROS, namely HO$^{\bullet}$ radicals.

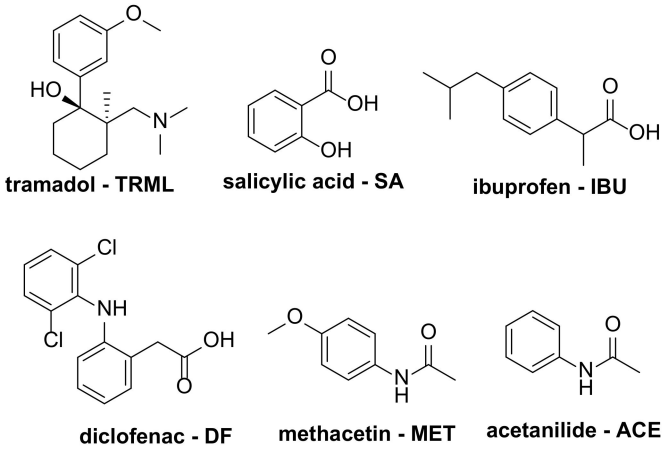

Figure 5. Structures of the analgesics herein discussed.

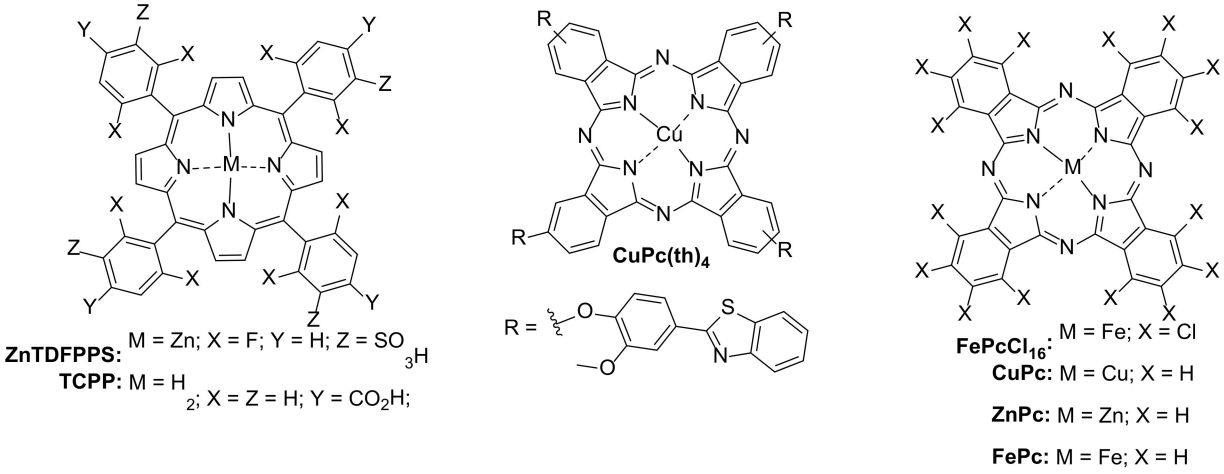

Figure 6. Structures of tetrapyrrolic macrocycles (TPM) used as photocatalysts for degradation of analgesics.

3.1. Photochemical Degradation

The Huang group used the iron complex of perchlorinated phthalocyanine, **$FePcCl_{16}$** (Figure 6) (Table 3, entry 2) [58], as a heterogeneous photocatalyst to promote the degradation of salicylic acid (**SA**, Figure 5) upon irradiation with visible light from a 500 W halogen lamp. A 70% **SA** degradation was achieved after 10 h irradiation, with a catalyst concentration of 0.4 g/L, using H_2O_2 as oxidant (3×10^{-3} M), with a kinetics of k_{obs} = 1.2×10^{-1} min^{-1}. Once again, the mechanism was attributed to the formation of $HO^{\bullet}$ radicals.

Anucha and Altin [15] developed the material **$CuPc(th)_4$@TiO_2/ZnO** by modifying TiO_2 and ZnO semiconductor blends with thiazol tetrasubstituted copper phthalocyanine (**$CuPc(th)_4$**, Figure 6). This hybrid material was evaluated on the photodegradation of ibuprofen (**IBU**, Figure 5) in an aqueous matrix using five mercury lamps of 40 W at 365 nm (Table 3, entry 3). Under these conditions, 80% of **IBU** photodegradation was achieved in 4 h at pH 6.5 and a degradation rate constant of k_{obs} = 7.0×10^{-3} min^{-1}, against 42% by TiO_2/ZnO semiconducting catalyst. The authors also investigated the catalyst's stability, and a small decline (77%) of **IBU** degradation started only after the fifth cycle run. The authors put in evidence that a hydroxyl radical ($HO^{\bullet}$) and superoxide anion ($O_2^{\bullet -}$) are the main ROS species involved in **IBU** degradation.

Table 3. Photochemical degradation of analgesic drugs using TPM-based catalysts.

#/Ref	Catalyst	Drug	Experimental Conditions	Comments
1 [57]	**ZnTDFPPS@TiO_2**	[**TRML**] = 10 mg/L	- Matrix: Distilled water - LED light 530 ± 20 nm - [**ZnTDFPPS@TiO_2**] = 0.67 g/L - pH = N/A; T = N/A - Pre-dark: N/A	- 80% **TRML** degradation in 60 min - TOC: N/A - k_{obs}: N/A - Mechanism: $HO^{\bullet}$ - Reutilization tests: N/A
2 [58]	**$FePcCl_{16}$**	[**SA**] = 70 mg/L	- Matrix: Distilled water - 500 W halogen lamp (λ ≥ 420 nm) - [**$FePcCl_{16}$**] = 0.4 g/L - [H_2O_2] = 3×10^{-3} M - Pre-dark for 30 min - pH = 7; T = 25 °C	- 70% **SA** removed in 600 min - TOC: N/A - $k_{obs} = 1.2 \times 10^{-1}$ min^{-1} - Mechanism: $HO^{\bullet}$ - Reutilization tests: N/A
3 [15]	**$CuPc(th)_4@TiO_2/ZnO$**	[**IBU**] = 5 mg/L	- Matrix: Distilled water - Mercury lamps 5 × 40 W (λ = 365 nm - [**$CuPc(th)_4@TiO_2/ZnO$**] = N/A (thin films of unknown Pc content) - pH = 6.5; T = 25 °C - Pre-dark for 30 min	- 80% IBU degradation in 240 min - TOC: N/A - $k_{obs} = 7.0 \times 10^{-3}$ min^{-1} - Mechanism: $HO^{\bullet}$ and $O_2^{\bullet-}$ - Reutilization: 5 cycles
4 [20]	**$CuPc@TiO_2$** **$ZnPc@TiO_2$**	[**IBU**] = 10 mg/L	- Matrix: Distilled water - 3 laser diodes 20 mW/cm^2 at λ = 365 nm (UV); at λ = 665 nm (Vis) - -[**$MPc@TiO_2$**] = 1 g/L - pH = N/A; T ≤ 35 °C	- 0% **IBU** degradation in 360 min (Vis) - 95% IBU degradation in 360 min (UV) with **$CuPc@TiO_2$** - 55% IBU degradation in 360 min (UV) with **$ZnPc@TiO_2$** - $k_{obs} = 3.8 \times 10^{-1}$ min^{-1} with **$CuPc@TiO_2$** - Mechanism: N/A - Toxicity assessment: increase in toxicity (10%) in oxidation products
5 [59]	**FePc@ZnO**	[**IBU**] = 20 mg/L	- Matrix: Distilled water - 300 W xenon lamp - [**FePc@ZnO**] = 0.5 g/L - [H_2O_2] = 10 mmol/L - pH = 6.5; T = 25 °C	- 90% IBU degradation in 10 min - TOC: N/A - k_{obs} = N/A - Mechanism: $HO^{\bullet}$ - Degradation pathway proposed - Reutilization: 5 cycles
6 [60]	**PCN-134 (TCPP@Zr-BTB MOF)**	[**DF**] = 30 mg/L	- Matrix: Distilled water - 500 W Xe lamp λ > 420 nm - -[**PCN-134**] = 0.1 g/L - pH = 7; T = 25 °C - Pre-dark for 30 min	- 99% **DF** degradation in 300 min - Mechanism: h^+ and $^1O_2$ (Type II) - Reutilization: 3 cycles
7 [61]	**TCPP@UiO-66 MOF**	[**DF**] = 30 mg/L	- Matrix: Distilled water - Simulated-sunlight 350 W Xe lamp (290 nm ≤ λ ≤ 1200 nm) - [**TCPP@UiO-66**] = 0.1 g/L pH = 7; T = 25 °C	- 99% **DF** degradation in 240 min - $k_{obs} = 8.4 \times 10^{-3}$ min^{-1} - Mechanism: h+ and $^1O_2$ (Type II) - Reutilization: 4 cycles

Mlynarczyk also investigated the **IBU** aqueous photodegradation in the presence of zinc(II) and copper(II) phthalocyanines (**ZnPc** and **CuPc**, respectively, Figure 6) embedded onto pure anatase-phase TiO_2 nanoparticles (**$ZnPc@TiO_2$** and **$CuPc@TiO_2$**) [20]. Catalyst photoactivity was evaluated on a 10 mg/L solution of **IBU** in water by irradiating with three lasers (20 mW/cm^2) under either UV (365 nm) or visible light (665 nm) (Table 3, entry 4). They obtained 95% **IBU** degradation with **$CuPc@TiO_2$** under UV light irradiation after 6 h and a rate constant $k_{obs} = 3.8 \times 10^{-1}$ min^{-1}, while using **$ZnPc@TiO_2$**, only 55%

degradation was observed (Figure 7a). Interestingly, this value is even lower than the one observed when **TiO_2** was used as catalyst, which reached nearly 93% photodegradation. On the other hand, negligible degradation was observed for both catalysts under visible-light irradiation, as can be seen in Figure 7b, which may be attributed to low light absorption by the catalyst.

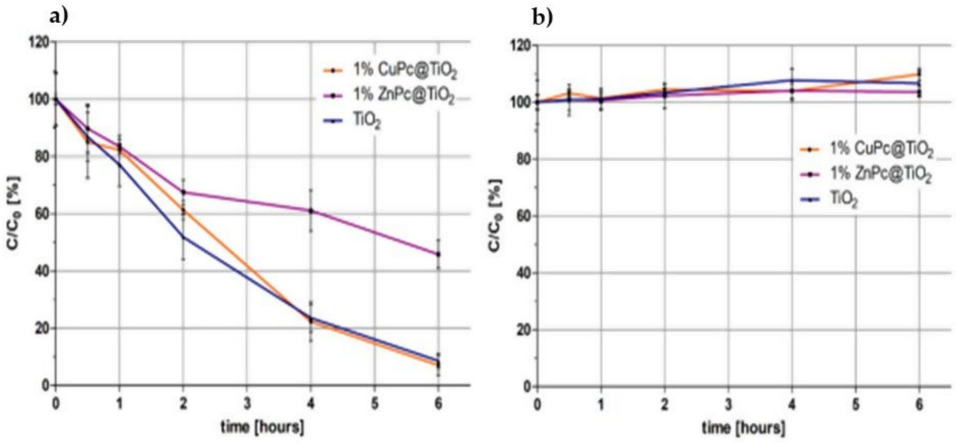

Figure 7. The changes in **IBU** concentration after irradiation of the solution containing photocatalyst at (**a**) 365 nm light and (**b**) 665 nm light. Adapted with permission from ref. [20]. Copyright 2020 MDPI.

Furthermore, Ju and Hou [59] prepared the photocatalyst **FePc@ZnO** by impregnation of FePc (Figure 6) onto semiconducting **ZnO**. The authors studied the photo-Fenton-type degradation of **IBU** (Figure 5) in the presence of the catalyst, using H_2O_2 as the oxidant and a visible-light Xe lamp (330 W) as the irradiation source. A 90% degradation of IBU was achieved in just 10 min, for which $HO^{\bullet}$ was found to be the main oxidation species. The catalysts showed reusability for up to five cycles without significant loss of activity (Table 3, entry 5).

Several groups studied the ability of TPM-based catalysts to degrade diclofenac (**DF**, Figure 5). Yu's group studied its photodegradation using two different porphyrin-based MOFs. In a first study, they prepared **PCN-134**, **TCPP@Zr-BTB** MOF [60] based on a *meso*-tetra(carboxyphenyl)porphyrin (**TCPP**, Figure 6) metal organic framework. After stirring a **DF** aqueous solution (30 mg/L) for 30 min in the dark to favor the adsorption-desorption equilibrium, the solution was irradiated with a visible-light Xe lamp (500 W) for 5 h, 99% of **DF** photodegradation was achieved using **PCN-134** as photocatalyst (0.1 g/L; Table 3, entry 6). Moreover, the authors established that the mechanism of **PCN-134** photodegradation is type II due to the generation of singlet oxygen ($^1O_2$). Additionally, the authors also performed catalyst-reutilization studies for three cycles, providing removal rates > 95%.

In a subsequent study, the same group developed another MOF-type catalyst, **TCPP@UiO-66** [61]. Particularly, **TCPP** (Figure 6) was introduced onto **UiO-66** crystals via an in situ solvothermal one-pot reaction, preserving the morphologic characteristics of **UiO-66**. Then, the authors irradiated a **DF** aqueous solution (30 mg/L) containing a catalyst concentration of 0.1 g/L, at pH 7, by simulated-sunlight 350 W Xe lamp (290 nm $\leq \lambda \leq$ 1200 nm) (Table 3, entry 7). Under these conditions, 99% of **DF** photodegradation was obtained after 4 h ($k_{obs} = 8.4 \times 10^{-3}$ min^{-1}). The catalyst showed good recyclability for four reaction cycles without loss activity. As in the previous study, the authors attributed the photodegradation of **DF** mainly to the generation of $^1O_2$, along with h^+ (holes), to a minor extent.

3.2. Oxidative Chemical Degradation

The degradation of **DF** (Figure 5) was also studied under nonphotochemical conditions. The Nackiewicz group studied the catalytic activity of iron(II) octacarboxyphthalo-

cyanine (**FeC8Pc**, Figure 8) in the homogenous oxidation of an aqueous solution of **DF** at pH 8, using H_2O_2 or $NaIO_4$ as oxidants (Table 4, entry 1) [55]. At a substrate/catalyst 50:1 molar ratio, the authors obtained full **DF** degradation in 35 min and 25 min when using H_2O_2 and $NaIO_4$, respectively. **FeC8Pc** also self-degraded completely due to the production of hydroxyl radicals formed by H_2O_2. The authors further studied the degradation pathway for **DF**, observing the generation of an unstable dimeric **DF** oxidation compound as intermediate, further leading to the final oxidation products.

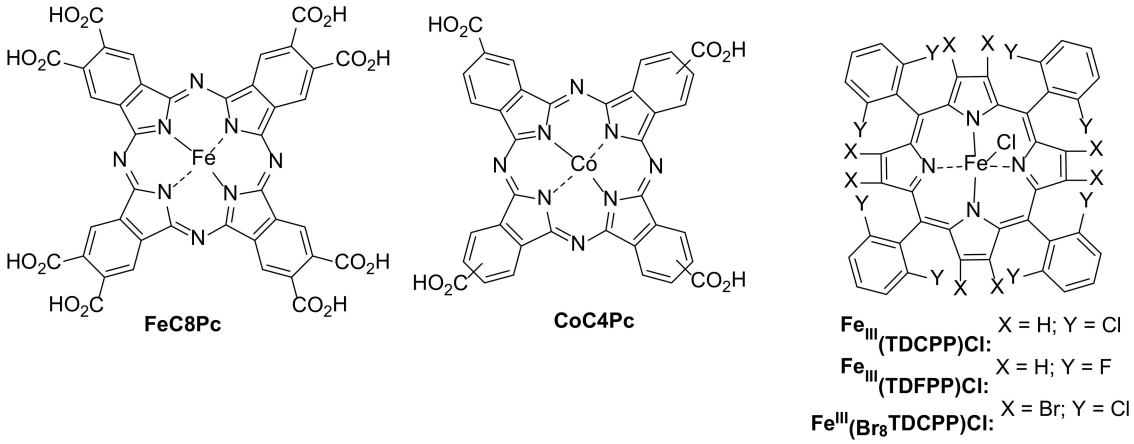

Figure 8. Structures of tetrapyrrolic macrocycles (TPM) used as catalysts for oxidative chemical degradation of analgesic pharmaceuticals.

Table 4. Nonphotochemical degradation of analgesic drugs using TPM-based catalysts.

#/Ref	Catalyst	Drug	Experimental Conditions	Comments
1 [55]	**FeC8Pc**	[**DF**] = 6 mg/L	- Matrix: Distilled water - Homogeneous reaction - pH = 8; T = 25 °C - [**FeC8Pc**] = 0.003 g/L - $[H_2O_2] = 3.52 \times 10^{-4}$ M - $[NaIO_4] = 3.52 \times 10^{-4}$ M	- Homogenous - 99% **DF** degradation in 35 min with H_2O_2 - 99% **DF** degradation in 25 min with $NaIO_4$ - Mechanism: $HO^{\bullet}$ - Degradation pathway proposed - Reutilization: N/A
2 [62]	**CoC4Pc@CNOMS**	[**DF**] = 10 mg/L	- Matrix: Distilled water - [**CoC4Pc@CNOMS**] = 0.1 g/L - [PMS] = 3.2×10^{-4} M - pH = 7; T = 25 °C	- 99% **DF** degradation in 20 min - $k_{obs} = 1.87 \times 10^{-1}$ min^{-1} - Mechanism: $HO^{\bullet}$, $SO_4^{\bullet-}$ and $^1O_2$ - Degradation pathway proposed - Reutilization: 4 cycles
3 [63]	**Fe^{III}(TDCPP)Cl** **Fe^{III}(TDFPP)Cl** **$Fe^{III}(Br_8$TDCPP)Cl**	[**MET**] = 60 g/L [**ACE**] = 60 g/L	- Matrix: 3:2 mixture ACN/^{i}PrOH - [**porphyrin**] = 5.4 g/L - [2-Mercaptopyrimidine] = 3.8 g/L - [mCPBA] = 0.4 M - 1:10:100:100 - pH = N/A; T = 25 °C	- Homogeneous - 85% **MET** degradation in 24 h, 45% **ACE** degradation in 24 (using **$Fe^{III}(Br_8$TDCPP**)Cl) - Degradation pathway proposed - Reutilization: N/A

The authors further proposed a degradation pathway for DF (Scheme 7). DF (m/z = 295) was oxidized by $HO^{\bullet}$ into m/z 311 and m/z 309. Their referred quinone's ability to form charge-transfer complexes through electron transfer from donor to acceptor allowed DF and m/z 309 to be transformed into cation (m/z 295) and anion (m/z = 309) radicals, forming a charge-transfer complex [55].

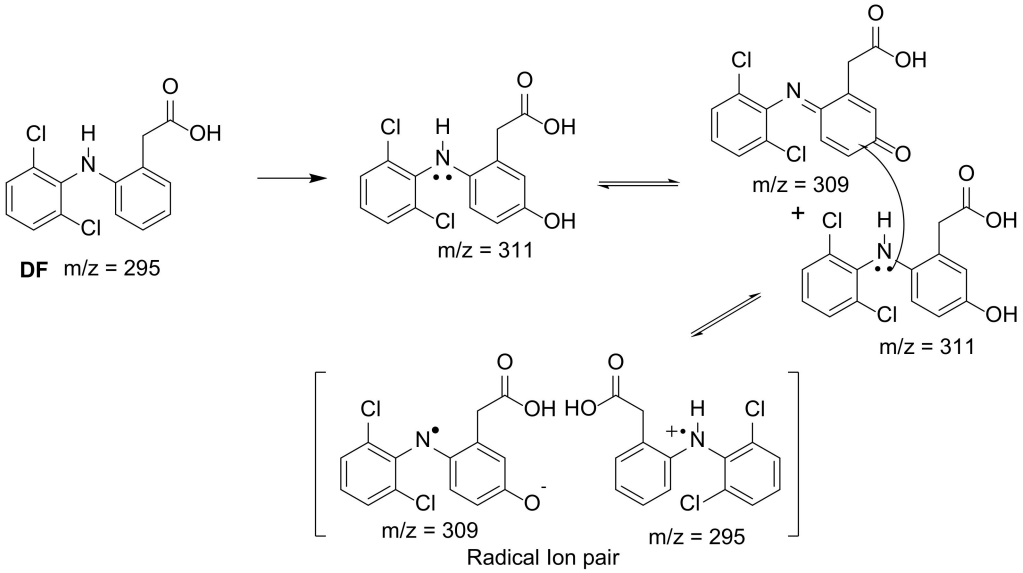

Scheme 7. Proposed pathway for the degradation of diclofenac [55].

Shi and Deng studied the catalytic performance of **CoC4Pc@CNOMS**, prepared by electrostatic linking of cobalt(II) tetracarboxyphthalocyanine (**CoC4Pc**, Figure 8) to an amino-functionalized manganese octahedral molecular sieve (**CNOMS**) on the degradation of a 10 mg/L **DF** aqueous solution, using PMS (3.2×10^{-4} M) as oxidant (Table 4, Entry 2) [62]. After a 20 min reaction, 99% of DF degradation was achieved, following a pseudo-first-order kinetics ($k_{obs} = 1.87 \times 10^{-1}$ min^{-1}). The authors observed that at pH = 7 and light activation of PMS, the degradation was promoted by both type I and type II mechanisms ($HO^{\bullet}$, $SO_4^{\bullet -}$ and $^1O_2$ ROS species). The catalyst was also reused in four cycles, and a continuous slight decrease in the activity was observed.

Jones's group studied the effect of several iron(III) porphyrins, chloro *meso*-tetra(2,6-dichlorophenyl)porphyrinate iron (**Fe^{III}(TDCPP)Cl**, Figure 8), chloro *meso*-tetra(2,6-difluorophenyl)porphyrinate iron (**Fe^{III}(TDFPP)Cl**, Figure 8) and chloro β-octabromo-*meso*-tetra(2,6-dichlorophenyl)porphyrinate iron (**Fe^{III}(Br_8TDCPP)Cl**, Figure 8), in the catalytic degradation of acetaminophen-derived drugs methacetin (**MET**, Figure 5) and acetanilide (**ACE**, Figure 5) (Table 4, entry 3) [63]. Using **Fe^{III}(Br_8TDCPP)Cl** as a catalyst (0.75 g/L) and mCPBA as oxidant (75 g/L), 85% **MET** and 45% **ACE** degradation, respectively, was achieved in 24 h. Moreover, they identified the oxidation metabolites by GC-MS, and the acetaminophen was the main product obtained in both experimental cases.

4. Degradation of Neurological Pharmaceuticals

Neurology drugs manage diseases, disorders and conditions that affect the brain and nervous system. Carbamazepine is the only known neurological-system pharmaceutical evaluated in TPM-based degradation studies (Figure 9). This psychotropic drug is commonly used to treat epilepsy. The mechanism of action involves the blocking of the sodium channels of the neuron's membranes. This drug is commonly found in wastewaters due to its frequent use and incomplete removal by the traditional processing methods. [64]

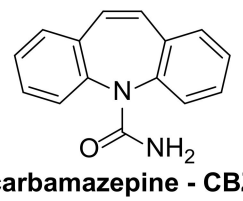

Figure 9. Structure of carbamazepine (**CBZ**).

4.1. Photochemical Degradation

The Lu and Chen group has been very active in the preparation of phthalocyanine-based ternary catalysts for the degradation of pharmaceuticals, namely carbamazepine (**CBZ**, Figure 9) [64–69]. They used zinc(II) tetra(carboxy)phthalocyanine (**ZnTCPc**, Figure 10) and blended it with polyacrylonitrile- (**PAN**) supported graphitic carbon nitride (g-C_3N_4), producing **ZnTCPc@g-C_3N_4/PAN** nanofibers (Table 5, entry 1,) [65]. The same phthalocyanine was also coupled with **g-C_3N_4** and enriched with graphene quantum dots (**GQD**), yielding the hybrid catalyst **ZnTCPc@g-C_3N_4/GQD** (Table 5, entry 2) [66]. When **CBZ** degradation tests were performed using **ZnTCPc@g-C_3N_4/PAN** and **ZnTCPc@g-C_3N_4/GQD** hybrid catalysts, **CBZ** was fully degraded in 5 h under visible-light Xe irradiation. However, in one case, [**CBZ**] = 2.5 mg/L and [**ZnTCPc@g-C_3N_4/PAN**] = 1 g/L (Table 5, entry 1) [65], while in the other experiment, the **CBZ** concentration was raised to 6 mg/L, with a catalyst concentration of just 0.1 g/L (25× higher substrate:catalyst ratio) (Table 5, entry 2) [66].

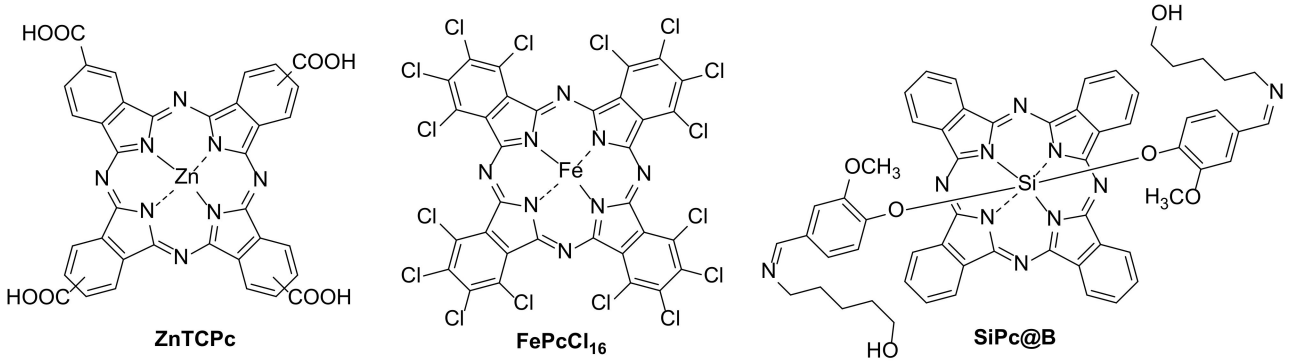

Figure 10. Structures of tetrapyrrolic macrocycles (TPM) mostly used as catalysts for degradation of carbamazepine.

Table 5. Photochemical degradation of neurologic pharmaceuticals using TPM-based catalysts.

#/Ref	Catalyst	Drug	Experimental Conditions	Comments
1 [65]	**ZnTCPc@g-C_3N_4/PAN nanofibers**	[**CBZ**] = 2.5 mg/L	- Matrix: Distilled water - Visible Light 100 W lamp λ > 400 nm - [**ZnTCPc@g-C_3N_4/PAN**] = 1 g/L - pH = N/A; T = 25 °C - Pre-dark: 10 min	- 98% **CBZ** degradation in 5 h - TOC: N/A - k_{obs}: N/A - Mechanism by h^+, $^1O_2$, $O_2^{\bullet-}$ - Reutilization: N/A - Degradation pathway proposed
2 [66]	**ZnTCPc@g-C_3N_4/GQD**	[**CBZ**] = 6 mg/L	- Matrix: Distilled water - Visible-light Xe solar simulator λ > 420 nm - [**ZnTCPc@g-C_3N_4/GQD**] = 0.1 g/L - pH = 5.3; T = 25 °C - Pre-dark: 10 min	- 99% **CBZ** degradation in 5 h - TOC: N/A - k_{obs}: N/A - Mechanism: by h^+, $^1O_2$, $O_2^{\bullet-}$ - Reutilization: N/A
3 [64]	**$FePcCl_{16}$**	[**CBZ**] = 6 mg/L	- Matrix: Distilled water - Visible-light Xe solar simulator λ > 420 nm - [**$FePcCl_{16}$**] = 0.1 g/L - [PMS] = 3×10^{-4} M or [H_2O_2] = 5×10^{-3} M - pH = 7; T = 25 °C	- 98% **CBZ** degradation in 90 min (using PMS) - < 10% **CBZ** degradation in 90 min (using H_2O_2) - TOC: 82% after 120 min - k_{obs}: 8.2×10^{-2} min^{-1} - Mechanism by $^1O_2$, $HO^{\bullet}$, $SO_4^{\bullet-}$ - Reutilization: 20 cycles - Degradation pathway proposed

Table 5. *Cont.*

#/Ref	Catalyst	Drug	Experimental Conditions	Comments
4 [67–69]	**$FePcCl_{16}$@g-C_3N_4-IMA** **$FePcCl_{16}$@g-C_3N_4-INA** **$FePcCl_{16}$@P_4VP/PAN**	[**CBZ**] = 6 mg/L	- Matrix: Distilled water - Visible-light Xe solar simulator λ > 420 nm - [**catalyst**] = 0.1–0.3 g/L - [PMS] = 3×10^{-4} M - pH = 7; T = 25 °C	- 98% **CBZ** degradation in 25 min - TOC: N/A - k_{obs}: N/A - Mechanism by $O_2^{\bullet-}$ and $^1O_2$ - Reutilization tests: N/A - Degradation pathway proposed
5 [14]	**$SiPc$@B/NaF-TiO_2**	[**CBZ**] = 10 mg/L	- Matrix: Distilled water - Visible-light 1500 W xenon lamp λ > 340 nm - [**$SiPc$@B/NaF-TiO_2**] = 1 g/L - pH = 6.5–6.9; T = 25 °C	- 70% **CBZ** degradation in 240 min - TOC: N/A - k_{obs}: 6.7×10^{-3} min^{-1} - Mechanism: N/A - Reutilization: N/A - Degradation pathway proposed

The same group further extended their studies of **CBZ** degradation, always using iron(II) hexadecachlorophthalocyanine (**$FePcCl_{16}$**, Figure 10) as TPM and oxone peroxymonosulfate (PMS) as oxidant. The authors performed studies with **$FePcCl_{16}$** [64] and by combining the phthalocyanine with **g-C_3N_4** through axial coordination, using isonicotinic acid (INA) [67] 1-methyl-*1H*-imidazole-5-carboxylic acid (IMA) [68] and poly (4-vinylpyridine)/polyacrylonitrile) (P_4VP/PAN) [69]. The corresponding catalysts, **$FePcCl_{16}$**, **$FePcCl_{16}$@g-C_3N_4-INA**, **$FePcCl_{16}$@g-C_3N_4-IMA** and **$FePcCl_{16}$@P_4VP/PAN**, were then used in the degradation of concentrated solutions of **CBZ** (6 mg/L) using a visible-light Xe-solar simulator in all experiments (Table 5, entries 3–4). The authors observed that heterogeneous but non-immobilized **$FePcCl_{16}$** provided a TOC of 82% after 120 min of reaction time, with a $k_{obs} = 8.2 \times 10^{-2}$ min^{-1}. This catalyst was reused along 20 cycles with no significant loss of activity (Table 5, entry 3) [64]. Then, they evaluated the effect of catalyst concentration onto **g-C_3N_4** (0.1 g/L–0.3 g/L), and the best result was achieved using **$FePcCl_{16}$@P_4VP/PAN** nanofibers (load = 0.3 g/L), with 98% in **CBZ** degradation (Table 5, entry 4) [68].

Furthermore, based on the intermediates of **CBZ** identified by authors using UPLC–HDMS, a possible degradation pathway was proposed, with h+, $O_2^{\bullet-}$ and $HO^{\bullet}$ being the main oxidizing species (Scheme 8). Firstly, the intermediates with m/z 253 were the initial photodegradation products of **CBZ** (m/z 237), subsequently undergoing a second $HO^{\bullet}$ addition to produce a dihydroxy-**CBZ** species with m/z 269 or the intermediate m/z 287. An alternative pathway would be the attack of the $O_2^{\bullet-}$ and $HO^{\bullet}$ on the olefinic double bond of the central seven-member ring, which resulted in the formation of 10,11-epoxy-**CBZ** (m/z 253). Additionally, a hydrogen-rearrangement reaction followed by the loss of the amide group could yield a compound with m/z 208, which could be further oxidized into acridine (m/z 180) or suffer the addition of $HO^{\bullet}$ to form an intermediate with m/z 224. Subsequently, the intermediate acridine could possibly further oxidize into the intermediate with m/z 196. All intermediates transformed to several biodegradable small molecules (below) [64–69].

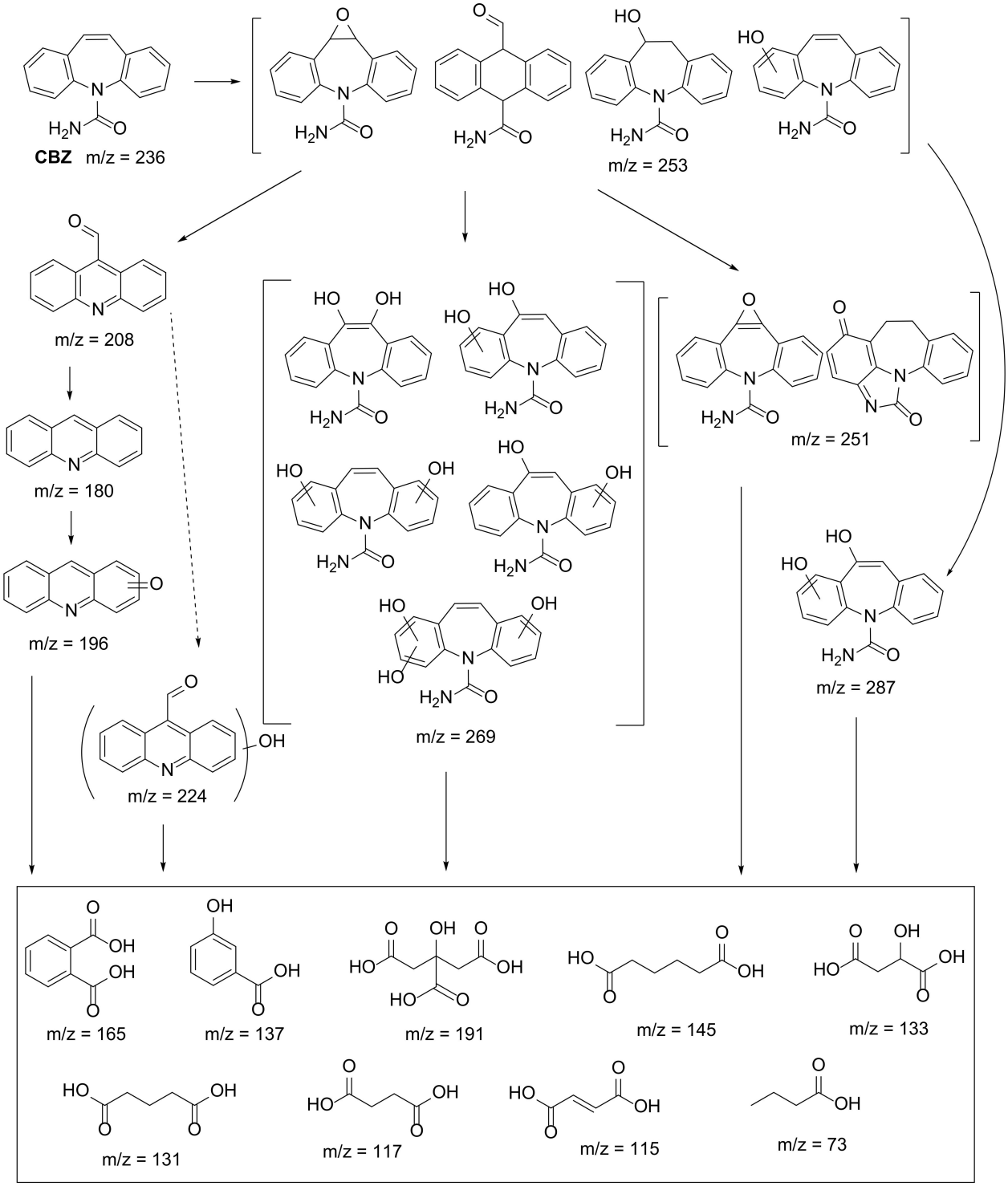

Scheme 8. Proposed degradation pathway for carbamazepine.

As peroxymonosulfate (PMS) was the oxidant used in all cases, sulfate ($SO_4^{\bullet -}$) and hydroxyl ($HO^{\bullet}$) radicals were the dominant active species in the oxidation catalytic process. As shown in Figure 11, the authors proposed that **$FePcCl_{16}$** could be induced to the excited state (***$FePcCl_{16}$**) under visible-light irradiation, then coordinating with the oxygen atoms of PMS to form a Fe(II)-O–O-SO_3^- species. The electron-donating effect of axial pyridine in **P4VP** can activate the heterolytic cleavage of the O–O bond and generate the high-valent iron-oxo (Fe^{IV}=O) species, which is proposed as the major active species in this reaction system [69].

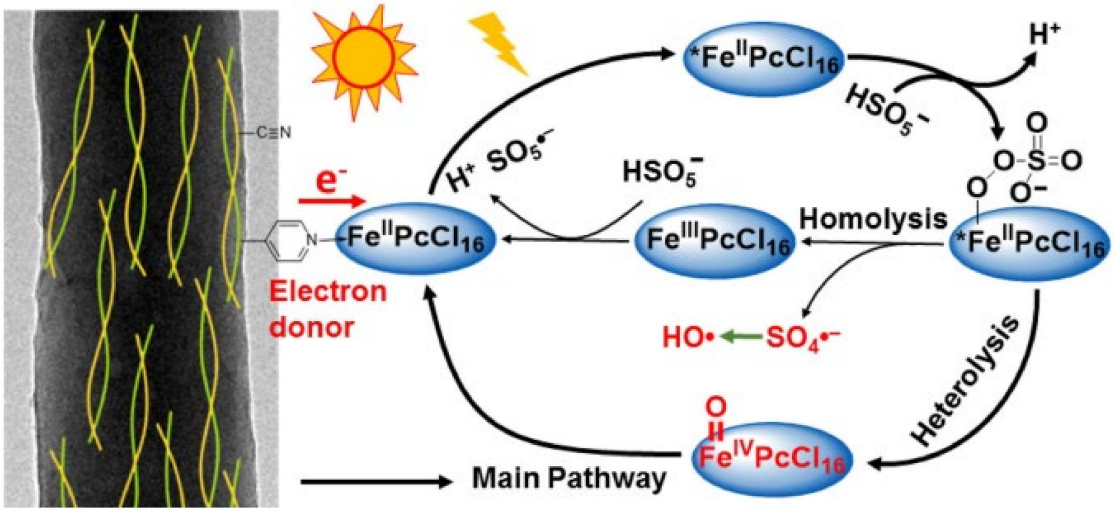

Figure 11. Proposed main pathway for the formation of active species when using **FePcCl$_{16}$-P$_4$VP/PAN** catalyst under visible-light irradiation (λ > 420 nm) in **CBZ** photodegradation. Adapted with permission from ref. [69]. Copyright 2019 Springer Nature.

Anucha [14] reported the synthesis of a hybrid catalyst consisting of a silicon phthalocyanine (**SiPc**, Figure 10) axially linked to a boron-sodium fluoride-doped TiO_2 semiconductor, producing the catalyst **SiPc@B/NaF-TiO$_2$** (Table 5, entry 5). The authors compared the effect of the support **B/NaF-TiO$_2$** with the hybrid catalyst, **SiPc@B/NaF-TiO$_2$** on the photodegradation of **CBZ** (10 mg/L) with visible light (1500 W xenon lamp λ > 340 nm). They observed that the support **B/NaF-TiO$_2$** provided the best result, with 70% degradation in 4 h (k_{obs} = 1.8 × 10^{-2} min^{-1}) [14,64–69].

4.2. Oxidative Chemical Degradation

Lu's group extended their exhaustive studies of **CBZ** degradation, using other phthalocyanine-based catalysts (Table 6, entries 1–3) [70–72] under Fenton-like oxidation conditions, using H_2O_2 as the oxidant. In a first study, the authors blended iron phthalocyanine (**FePc**, Figure 12) onto polyacrylonitrile (**PAN**), obtaining **FePc@PAN** nanofibers [70]. This catalyst, in a 1 g/L load, was then used in the degradation of **CBZ** (6 mg/L) in the presence of H_2O_2 (20 mM) at pH = 3 and temperature = 70 °C (Table 6, entry 1). The authors proposed that the hydroxyl (HO$^\bullet$) radicals were the dominant active species in the oxidation catalytic process. The catalyst could be reused eight times without significant loss of activity. Later, the same group tested the iron(II) hexadecafluorinated phthalocyanine μ-oxo dimer **(FePcF$_{16}$)$_2$O** (Figure 12) as catalyst for **CBZ** degradation, again using H_2O_2 as oxidant [71]. In a 0.1 g/L catalyst concentration and 20 mM H_2O_2, a 6 mg/L solution of **CBZ** was fully degraded in 40 min, regardless of the pH tested (Table 6, entry 2). By electron paramagnetic resonance and electrospray ionization–mass spectrometry, the authors proposed that the Fe^{IV}=O is the main active species arising from heterolytic cleavage of Fe^{III}–OOH species. Similar results were obtained later [72] using the same phthalocyanine μ-oxo dimer **(FePcF$_{16}$)$_2$O** (Figure 12) impregnated onto MWCNTs, providing the hybrid catalyst **(FePcF$_{16}$)$_2$O@MWCNT** (Table 6, entry 3). The system **(FePcF$_{16}$)$_2$O@MWCNT**/H_2O_2 (0.2 g/L and 5 mM, respectively) was also used to degrade **CBZ**, reaching full degradation in 60 min. Reutilization studies showed that the catalyst is active along 10 reutilization cycles. [70–72].

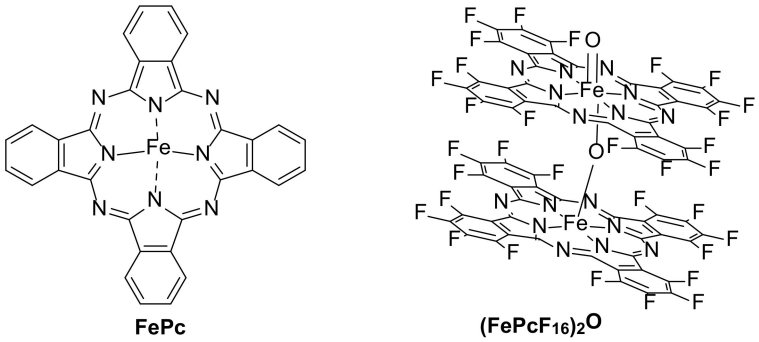

Figure 12. Structures of tetrapyrrolic macrocycles (TPM) used as catalysts for degradation of carbamazepine.

Table 6. Oxidative chemical degradation of neurological-system pharmaceuticals using TPM-based catalysts.

#/Ref	Catalyst	Drug	Experimental Conditions	Comments
1 [70]	**FePc@PAN**	[**CBZ**] = 6 mg/L	- Matrix: Distilled water - [**FePc@PAN**] = 1 g/L - [H_2O_2] = 2.0 × 10^{-2} M - pH = 3; T = 70 °C	- 99% **CBZ** degradation in 90 min - Mechanism by $HO^{\bullet}$ - TOC: N/A - k_{obs}: N/A - Reutilization: 8 cycles - Degradation pathway proposed
2 [71]	**(FePcF$_{16}$)$_2$O**	[**CBZ**] = 6 mg/L	- Matrix: Distilled water - [**(FePcF$_{16}$)$_2$O**] = 0.1 g/L - [H_2O_2] = 2.0 × 10^{-2} M - pH = 3, 5, 7 and 9; T = 30 °C	- 99% **CBZ** degradation in 40 min (at all pH) - Mechanism by Fe^{IV}=O - TOC: N/A - k_{obs}: 6.5 × 10^{-3} min^{-1} - Reutilization: N/A - Degradation pathway proposed
3 [72]	**(FePcF$_{16}$)$_2$O@MWCNT**	[**CBZ**] = 6 mg/L	- Matrix: Distilled water - [**(FePcF$_{16}$)$_2$O@MWCNT**]= 0.2 g/L - [H_2O_2] = 5 × 10^{-3} M - pH = 7; T = 30 °C	- 99% **CBZ** degradation in 60 min - Mechanism by Fe^{IV}=O - TOC: N/A - k_{obs}: N/A - Reutilization: 10 cycles - Degradation pathway proposed

5. Degradation of Miscellaneous Pharmaceuticals

Other miscellaneous drugs have been also evaluated in environmental degradation studies.

Limson studied the degradation of regulatory hormones estrone (**E1**, Figure 13) and estradiol (**E2**, Figure 13), using unsubstituted manganese(II) and iron(II) phthalocyanines (**MnPc** and **FePc**, respectively, Figure 14) [73]. When **MnPc** was used (6.8 mg/L), both **E1** and **E2** (8 mg/L) were almost fully degraded, using H_2O_2 as oxidant (0.56 mM) at pH = 3, in 30 min (Table 7, entry 1).

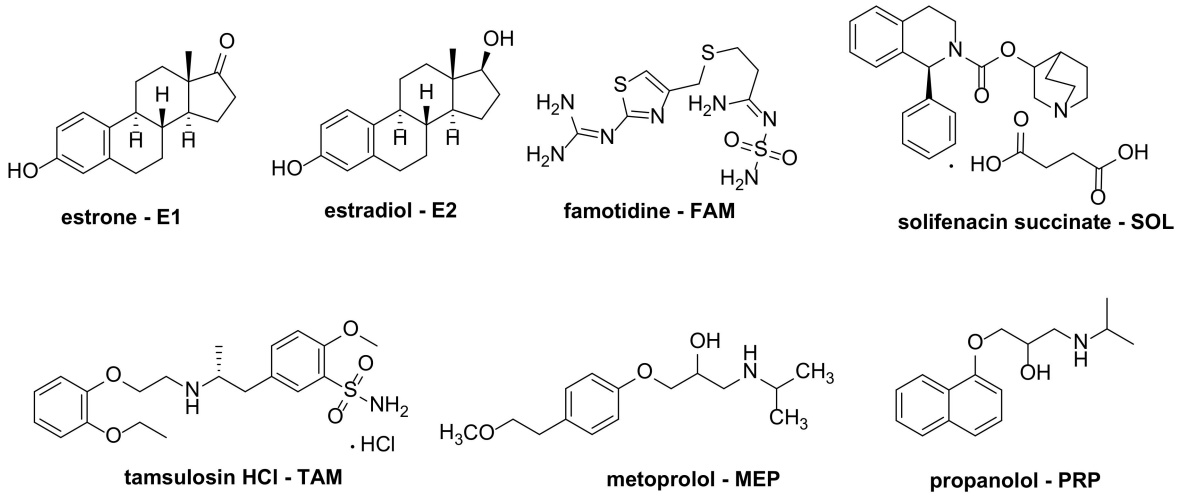

Figure 13. Structures of miscellaneous pharmaceuticals.

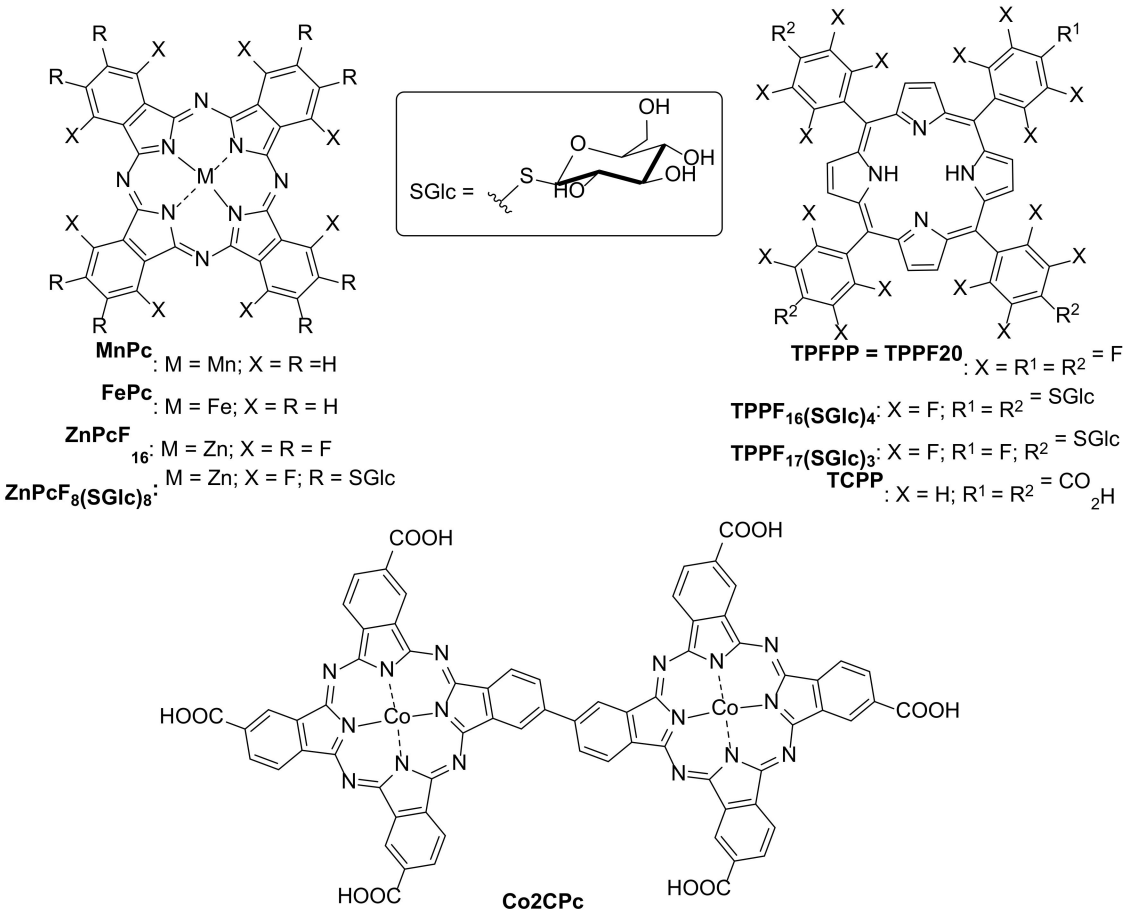

Figure 14. Structures of tetrapyrrolic macrocycles (TPM) used as catalysts for degradation of miscellaneous pharmaceuticals.

Tomé [74] reported the preparation of hybrid catalysts **TPPF$_{20}$@MNP**, **TPPF$_{16}$(SGlc)$_4$ @MNP**, **TPPF$_{17}$(SGlc)$_3$@MNP**, **ZnPcF$_{16}$@MNP** and **ZnPcF$_8$(SGlc)$_8$@MNP** via covalent linkage of *meso*-substituted porphyrins (**TPPF$_{20}$**, **TPPF$_{16}$(SGlc)$_4$** and **TPPF$_{17}$(SGlc)$_3$**, Figure 14) and phthalocyanines (**ZnPcF$_{16}$** and **ZnPcF$_8$(SGlc)$_8$**, Figure 14) to aminopropyl-functionalized silica-coated magnetic nanoparticles (MNP)(Table 7, entry 2). These catalysts were evaluated in the photodegradation of estradiol (**E2**, Figure 13), and the best results were obtained with **TPPF$_{17}$(SGlc)$_3$@MNP** and **ZnPcF$_8$(SGlc)$_8$@MNP**), reaching

82% degradation of **E2** after 8 h irradiation with a visible-light white lamp (4 mW/cm^2. The authors obtained better results (100% **E2** degradation) under flow conditions with a residence time of 60 min. The authors attributed this higher efficiency in flow mode to the better penetration of light into the suspension since the narrowness of the tube allowed a much more efficient irradiation.

Table 7. Summary of miscellaneous pharmaceuticals' degradation processes using TPM-based catalysts.

#/Ref	Catalyst	Drug	Experimental Conditions	Comments
1 [73]	**FePc** **MnPc**	[**E1**] = 8 mg/L [**E2**] = 8 mg/L	- Matrix: phosphate buffer (50 mM) + 30% *v*/*v* MeCN - -[**MnPc**] = 6.8 mg/L, [H_2O_2] = 5.6 × 10^{-4} M, pH = 3 - -[**FePc**] = 1.3 mg/L, [H_2O_2] = 3 × 10^{-3} M, - pH = 7, T = 35 °C	- 100% **E1** degradation in 30 min (both catalysts) - -100% **E2** degradation with **MnPc** and 91% **E2** degradation with **FePc** (in 30 min) - TOC: N/A - k_{obs}: N/A - Reutilization: N/A
2 [74]	**$TPPF_{20}$@MNP** **$TPPF_{16}(SGlc)_4$@MNP** **$TPPF_{17}(SGlc)_3$@MNP** **$ZnPcF_{16}$@MNP** **$ZnPcF_8(SGlc)_8$@MNP**	[**E2**] = 5 mg/L	- Matrix: Distilled water - White visible-light lamp (4 mW/cm^2) - [**MNP-catalyst**] = ~0.1 g/L to ~0.2 g/L - pH = 4, 6 and 8; T = 25 °C - Pre-dark for 1 h	- 82% **E2** degradation with **$TPPF_{17}(SGlc)_3$@MNP** or **$ZnPcF_8(SGlc)_8$@MNP** (batch—8 h) - 100% **E2** degradation with **$TPPF_{17}(SGlc)_3$@MNP** (flow—1 h) - Mechanism: mainly by $^1O_2$ - TOC: N/A - k_{obs}: for **$TPPF_{17}(SGlc)_3$@MNP** (5.7 × 10^{-2} min^{-1} in flow) - Reutilization: 3 cycles in batch
3 [22]	**$TCPP@TiO_2$**	[**FAM**] = 28 mg/L [**SOL**] = 30 mg/L [**TAM**] = 34 mg/L	- Matrix: Distilled water - 500 W halogen lamp - [**$TCPP@TiO_2$**] = 0.3 g/L - pH = N/A; T = 25 °C - Pre-dark: 30 min	- 100% **FAM** removed in 180 min. - < 10% for **SOL** and **TAM** in 180 min - TOC: N/A - reutilization on **FAM** decreased degradation to 65% - Degradation pathway proposed for all drugs
4 [75]	**TCPP@ATiNT** **TCPP@Si-ATiNT**	[**FAM**] = 100 mg/L	- Matrix: Distilled water - UV-light 150 W mercury lamp 248 nm < λ < 579 nm - Visible-light 500 W halogen lamp - [catalysts] = 0.25 g/L - pH = N/A; T = N/A - Pre-dark: 1 h	- using **TCPP@Si-ATiNT**: 60% degradation upon UV irradiation in 240 min and 80% degradation upon Visible irradiation in 240 min. - using **TCPP@ATiNT**: 99% degradation upon Visible irradiation in 240 min. - TOC: N/A - Mechanism: by h^+ - k_{obs} = 8.0 × 10^{-3} min^{-1} by **TCPP@Si-ATiNT** - k_{obs} = 21.7 × 10^{-3} min^{-1} by **TCPP@ATiNT** - Reutilization: N/A
5 [76]	**$TPFPP@NH_2$-SiO_2**	[**MEP**] = 50 mg/L	- Matrix: Distilled water, wastewater - Solar-simulator 1550 W arc xenon lamp 295 nm < λ < 400 nm - Direct sunlight - [**$TPFPP@NH_2$-SiO_2**] = 2.5 g/L - pH = 7.5; T = 25 °C	- 63% **MEP** degradation in 12 h (solar simulator, distilled water) - 58 % **MEP** degradation in 6 h (sunlight, distilled water) - 60% **MEP** degradation in 12 h (solar simulator, wastewater) - TOC = N/A - k_{obs} = 6.5 × 10^{-3} min^{-1} (solar simulator, distilled water) - Mechanism by $^1O_2$ - Reutilization: N/A - Degradation pathway proposed

Table 7. *Cont.*

#/Ref	Catalyst	Drug	Experimental Conditions	Comments
6 [77]	**Co_2CPc@CNOMS**	[**PRP**] = 5 mg/L	- Matrix: Distilled water - [**Co_2CPc@CNOMS**] = 0.1 g/L - -[PMS] = 3.2×10^{-4} M - pH = ~6; T = 25 °C	- 93% **PRP** degradation in 30 min - 47% TOC in 30 min - $k_{obs} = 9.2 \times 10^{-2}$ min^{-1} - Mechanism by $SO_4^{\bullet -}$ and $^1O_2$ - Reutilization: 4 cycles - Degradation pathway proposed

Nolan [22] prepared the hybrid catalyst **TCPP@TiO_2** by adsorbing *meso*-tetra(4-carboxyphenyl)porphyrin (**TCPP**, Figure 14) onto TiO_2. Three pharmaceuticals were tested (famotidine (**FAM**), solifenacin succinate (**SOL**) and tamsulosin HCl (**TAM**); Figure 13) in 0.083 mM solutions (28 mg/L, 30 mg/L and 34 mg/L for **FAM**, **SOL** and **TAM**, respectively) under irradiation with a 500 W visible-light halogen lamp (Table 7, entry 3). Under these conditions, only **FAM** was fully degraded (100%) after 180 min, while the other pharmaceuticals gave less than 10% degradation products. Additionally, the authors mentioned that after the second cycle, a drop in **FAM** degradation to 65% was observed.

Chetty [75] used the same porphyrin (**TCPP**, Figure 14) to prepare the hybrid photocatalysts **TCPP@ATiNT** and **TCPP@Si-ATiNT** by immobilizing it onto anatase titanium nanotubes (**ATiNT**) and **Si-ATiNT** (Table 7, entry 4). The authors irradiated 100 mg/L of **FAM** aqueous solutions, using both a 150 W UV-light mercury lamp and a 500 W visible-light halogen lamp containing both catalysts in concentrations of 0.25 g/L. The authors concluded that **TCPP@ATiNT** was the best catalyst to promote full **FAM** degradation upon 240 min of irradiation, as demonstrated by its higher kinetic rate, $k_{obs} = 21.7 \times 10^{-3}$ min^{-1} against $k_{obs} = 8.0 \times 10^{-3}$ min^{-1}, when **TCPP@Si-ATiNT** was used. This difference was ascribed to the higher recombination rate favored by the silane-linker group present in the **TCPP@Si-ATiNT** catalyst, with a consequent decrease in electron injection. The authors also suggested that h+ holes formed in the HOMO of **TCPP** upon photoexcitation may be the most relevant oxidizing agent, rather than $^1O_2$, once photocatalytic experiments under oxygen-deficient conditions showed a similar rate of **FAM** degradation (Figure 15).

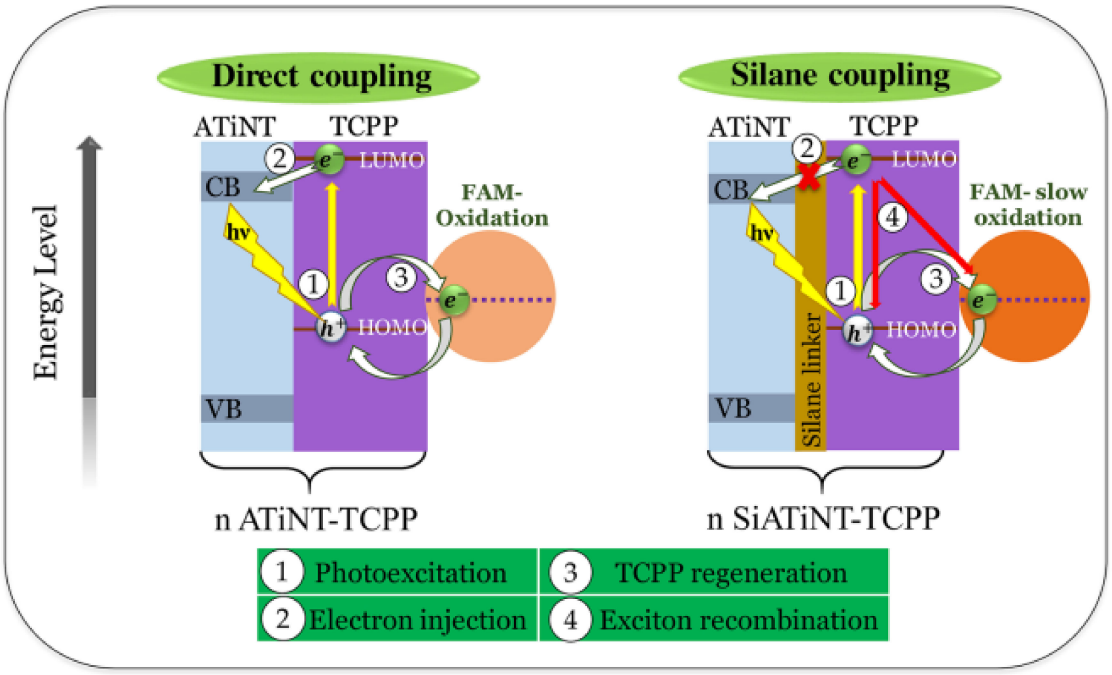

Figure 15. Schematic illustration of the proposed visible-light photocatalysis mechanism for **FAM** degradation using **TCPP@ATiNT** and **TCPP@Si-ATiNT**. Adapted with permission from ref [75]. Copyright 2020 Elsevier.

Other β-blocker pharmaceuticals like propranolol (**PRP**, Figure 13) and metoprolol (**MEP**, Figure 13) have been also studied by Neves and Simões [76], using *meso*-tetrakis(pentafluorophenyl)porphyrin (**TPFPP**, Figure 14) covalently immobilized onto amino functionalized silica oxide (**NH_2-SiO_2**) as heterogeneous catalyst (**TPFPP@NH_2-SiO_2**). **MEP** photodegradation was carried out using both a solar simulator and direct-sunlight irradiation. After 12 h, 63% and 58% **MEP** degradation was obtained, respectively (Table 7, entry 5).

Regarding the degradation of **PRP** with PMS (0.2 g/L) as oxidant, Huiping [77] described the synthesis of a catalyst based on a binuclear cobalt carboxyl-substituted phthalocyanine (**Co_2CPc**, Figure 14) supported by electrostatic interactions onto amino-functionalized manganese octahedral molecular sieves (**CNOMS**) (Table 7, entry 6). A 93% **PRP** degradation (k_{obs} = 9.2 × 10^{-2} min^{-1}) was observed after 30 min, and 47% TOC. The authors proposed that both $SO_4^{\bullet -}$ radicals and $^1O_2$ were the main oxidation species. Furthermore, reutilization was performed, and the catalyst remained active and stable for four cycles, as shown in Figure 16.

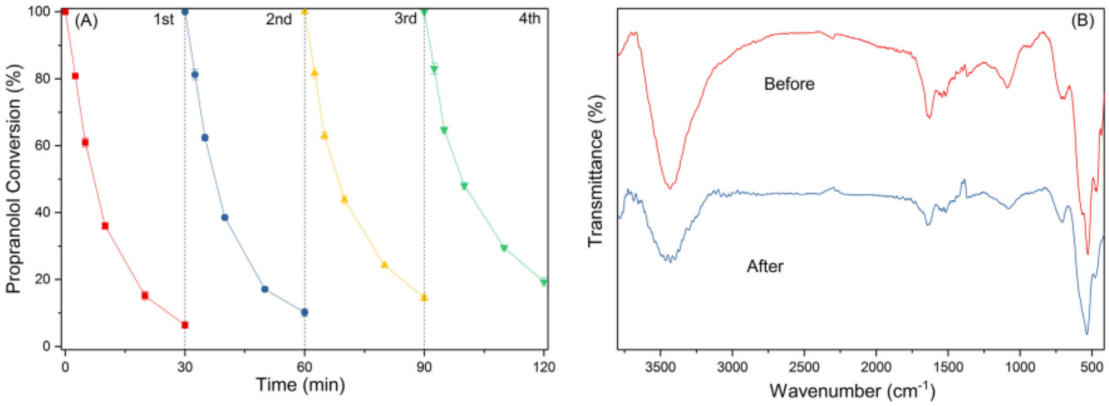

Figure 16. (**a**) Reutilization cycles for **PRP** degradation; (**b**) FT-IR spectra of **Co_2CPc@NOMS-2** before and after the reutilization cycles. Adapted with permission from ref. [77]. Copyright 2019 Elsevier.

6. Conclusions and Perspectives

Considering the literature herein reviewed, one can generally conclude that the scientific community has been committed to finding more sustainable and alternative catalytic processes for the degradation of pharmaceuticals in the environment, particularly using tetrapyrrole macrocycle- (TPM) based catalysts. The main parameters requiring attention when developing such a catalytic system aiming its transposition at real-world application must include:

(i) the TPM, considering its modulability and functionality, including substitution patterns for activity/stability;
(ii) the type of support, aiming preferential immobilization at efficient reutilization and/or the holding of suitable semiconducting characteristics;
(iii) the light source, when designing a photocatalytic system, preferentially using visible/solar energy;
(iv) the oxidants, when designing oxidative chemical systems, giving preference to environmentally benign ones.

The most relevant examples discussed above can be highlighted by, for instance, the **TNCuPc@CeO_2/Bi_2MoO_6** (copper(II) β-tetranitrophthalocyanine deposited on the surface of semiconducting **CeO_2/Bi_2MoO_6** nanoflowers), which, when used in 1.5 g/L concentration, showed high catalytic performance in the photodegradation of antibiotic tetracycline (0.05 g/L concentration), with reusability up to four cycles without significant

loss of activity, reaching, after 120 min irradiation with 800 W xenon visible light, a TOC removal efficiency of 83%, one of the highest reported so far [21].

In another relevant study, a porphyrin-MOF-type catalyst (**TCPP@UiO-66**), prepared by introducing *meso*-tetra(carboxyphenyl)porphyrin (**TCPP**) onto **UiO-66** crystals, was used to degrade a diclofenac aqueous solution (0.03 mg/L) containing a catalyst concentration of 0.1 g/L, reaching complete photodegradation when irradiated by a simulated-sunlight 350 W Xe lamp (290 nm $\leq \lambda \leq$ 1200 nm) and showing good recyclability [61].

For oxidative chemical degradation systems, the use of an **MnTDCPPS@N-SiO$_2$** catalyst (*meso*-tetrakis(2,6-dichloro-3-sulfophenyl)porphyrinato manganese(III) covalently attached to aminopropyl functionalized silica gel) in the degradation of recalcitrant trimethoprim antibiotic must be highlighted. The immobilized catalyst, notwithstanding its use in quite a low concentration (0.002 g/L) and in the presence of 0.26 mM H_2O_2 as oxidant, was able to promote the oxidative degradation of trimethoprim (0.13 g/L) in 95% (24% TOC decrease) after 150 min, showing reusability for up to five cycles without losing its activity [54].

As a whole, efforts in the design and larger-scale preparation of efficient catalysts should point to the modulation/functionalization of TPMs holding appropriate substituent-imparting catalyst stability (e.g., bearing electron-withdrawing groups at the periphery) and suitable functionalities to promote covalent immobilization to supports, therefore avoiding catalyst leaching upon reutilization. When developing photocatalytic systems, these should aim for longer wavelength absorption and lower-charge carrier recombination (when using semiconductors as supports), where solar energy irradiation sources should be preferred. On the other hand, oxidants should be of primary concern when using catalysts for chemical oxidation, giving preference to benign sources, such as molecular oxygen, hydrogen peroxide or potassium peroxymonosulfate.

Another important challenge concerns the achievement of complete degradation of pharmaceuticals. When only partial/low mineralization occurs (the large majority of the studies herein reported), we consider that it is crucial to evaluate the byproducts generated to ensure their lower toxicity and environmental persistence since they can also contribute to increase the environmental toxicity and, particularly, the development of multi-resistant bacteria when dealing with antibiotics.

Author Contributions: Conceptualization, M.J.F.C. and M.M.P.; methodology, G.P., R.T.A. and M.M.P.; formal analysis, M.M.P.; writing—original draft preparation, G.P., R.T.A., F.M.S.R., R.M.B.C., S.M.A.P., M.J.F.C. and M.M.P.; writing—review and editing, G.P., R.T.A., R.M.B.C., M.J.F.C. and M.M.P.; supervision, M.J.F.C. and M.M.P.; funding acquisition, M.M.P. All authors have read and agreed to the published version of the manuscript.

Funding: The authors acknowledge funding by FCT (Fundação para a Ciência e Tecnologia), QREN/FEDER (COMPETE Programa Operacional Factores de Competitividade) for projects UIDB/00313/2020 and PTDC/QUI-OUT/27996/2017 (DUALPI). Giusi Piccirillo thanks FCT for PhD grant PD/BD/135532/2018. Rafael T. Aroso thanks FCT for PhD grant PD/BD/143123/2019.

Conflicts of Interest: The authors declare no conflict of interest.

References

1. Calvete, M.J.F.; Piccirillo, G.; Vinagreiro, C.S.; Pereira, M.M. Hybrid Materials for Heterogeneous Photocatalytic Degradation of Antibiotics. *Coord. Chem. Rev.* **2019**, *395*, 63–85. [CrossRef]
2. Kutuzova, A.; Dontsova, T.; Kwapinski, W. Application of Tio2-Based Photocatalysts to Antibiotics Degradation: Cases of Sulfamethoxazole, Trimethoprim and Ciprofloxacin. *Catalysts* **2021**, *11*, 728. [CrossRef]
3. Ye, S.J.; Zeng, G.M.; Wu, H.P.; Zhang, C.; Liang, J.; Dai, J.; Liu, Z.F.; Xiong, W.P.; Wan, J.; Xu, P.A.; et al. Co-Occurrence and Interactions of Pollutants, and Their Impacts on Soil Remediation—A Review. *Crit. Rev. Environ. Sci. Technol.* **2017**, *47*, 1528–1553. [CrossRef]
4. Guo, Q.; Zhou, C.Y.; Ma, Z.B.; Ren, Z.F.; Fan, H.J.; Yang, X.M. Elementary Photocatalytic Chemistry on TiO_2 Surfaces. *Chem. Soc. Rev.* **2016**, *45*, 3701–3730. [CrossRef]
5. Nosaka, Y.; Nosaka, A.Y. Generation and Detection of Reactive Oxygen Species in Photocatalysis. *Chem. Rev.* **2017**, *117*, 11302–11336. [CrossRef] [PubMed]

6. Reddy, P.A.K.; Reddy, P.V.L.; Kwon, E.; Kim, K.-H.; Akter, T.; Kalagara, S. Recent Advances in Photocatalytic Treatment of Pollutants in Aqueous Media. *Environ. Int.* **2016**, *91*, 94–103. [CrossRef] [PubMed]
7. Opoku, F.; Govender, K.K.; van Sittert, C.G.C.E.; Govender, P.P. Recent Progress in the Development of Semiconductor-Based Photocatalyst Materials for Applications in Photocatalytic Water Splitting and Degradation of Pollutants. *Adv. Sustain. Syst.* **2017**, *1*, 1700006. [CrossRef]
8. Fernández, L.; Esteves, V.I.; Cunha, Â.; Schneider, R.J.; Tomé, J.P.C. Photodegradation of Organic Pollutants in Water by Immobilized Porphyrins and Phthalocyanines. *J. Porphyr. Phthalocyanines* **2016**, *20*, 150–166. [CrossRef]
9. Nonell, S.; Flors, C. (Eds.) *Singlet Oxygen: Applications in Biosciences and Nanosciences*; Comprehensive Series in Photochemical & Photobiological Sciences; RSC Books: Cambridge, UK, 2016; Volume 1.
10. Wiehe, A.; O'Brien, J.M.; Senge, M.O. Trends and Targets in Antiviral Phototherapy. *Photochem. Photobiol. Sci.* **2019**, *18*, 2565–2612. [CrossRef]
11. Diaz-Uribe, C.E.; Vallejo-L., W.A.; Miranda, J. Photo-Fenton Oxidation of Phenol with Fe(Iii)-Tetra-4-Carboxyphenylporphyrin/Sio2 Assisted with Visible Light. *J. Photochem. Photobiol. A* **2014**, *294*, 75–80. [CrossRef]
12. Guerra-Rodriguez, S.; Rodriguez, E.; Singh, D.N.; Rodriguez-Chueca, J. Assessment of Sulfate Radical-Based Advanced Oxidation Processes for Water and Wastewater Treatment: A Review. *Water* **2018**, *10*, 1828. [CrossRef]
13. Gao, W.; Tian, J.; Fang, Y.; Liu, T.; Zhang, X.; Xu, X.; Zhang, X. Visible-Light-Driven Photo-Fenton Degradation of Organic Pollutants by a Novel Porphyrin-Based Porous Organic Polymer at Neutral Ph. *Chemosphere* **2020**, *243*, 125334. [CrossRef]
14. Anucha, C.B.; Altin, I.; Fabbri, D.; Degirmencioglu, I.; Calza, P.; Magnacca, G.; Stathopoulos, V.N.; Bacaksiz, E. Synthesis and Characterization of B/Naf and Silicon Phthalocyanine-Modified TiO_2 and an Evaluation of Their Photocatalytic Removal of Carbamazepine. *Separations* **2020**, *7*, 71. [CrossRef]
15. Anucha, C.B.; Altin, I.; Bacaksiz, E.; Degirmencioglu, I.; Kucukomeroglu, T.; Yilmaz, S.; Stathopoulos, V.N. Immobilized TiO_2/ZnO Sensitized Copper (II) Phthalocyanine Heterostructure for the Degradation of Ibuprofen under Uv Irradiation. *Separations* **2021**, *8*, 24. [CrossRef]
16. Da Silva, T.H.; Ribeiro, A.O.; Nassar, E.J.; Trujillano, R.; Rives, V.; Vicente, M.A.; de Faria, E.H.; Ciuffi, K.J. Kaolinite/TiO_2/Cobalt(II) Tetracarboxymetallophthalocyanine Nanocomposites as Heterogeneous Photocatalysts for Decomposition of Organic Pollutants Trimethoprim, Caffeine and Prometryn. *J. Braz. Chem. Soc.* **2019**, *30*, 2610–2623. [CrossRef]
17. Gaeta, M.; Sanfilippo, G.; Fraix, A.; Sortino, G.; Barcellona, M.; Oliveri Conti, G.; Fragalà, M.E.; Ferrante, M.; Purrello, R.; D'Urso, A. Photodegradation of Antibiotics by Noncovalent Porphyrin-Functionalized TiO_2 in Water for the Bacterial Antibiotic Resistance Risk Management. *Int. J. Mol. Sci.* **2020**, *21*, 3775. [CrossRef] [PubMed]
18. Hu, K.; Chen, C.; Zhu, Y.; Zeng, G.; Huang, B.; Chen, W.; Liu, S.; Lei, C.; Li, B.; Yang, Y. Ternary Z-Scheme Heterojunction of Bi_2WO_6 with Reduced Graphene Oxide (rGO) and Meso-Tetra (4-Carboxyphenyl) Porphyrin (TCPP) for Enhanced Visible-Light Photocatalysis. *J. Colloid Interface Sci.* **2019**, *540*, 115–125. [CrossRef] [PubMed]
19. Huang, Y.; Zhao, P.; Miao, H.; Shao, S.; Wang, L.; Chen, Y.; Jia, C.; Xia, J. Organic-Inorganic Tcpp/Biocl Hybrids with Accelerated Interfacial Charge Separation for Boosted Photocatalytic Performance. *Colloids Surf. A Physicochem. Eng. Asp.* **2021**, *616*, 126367. [CrossRef]
20. Krakowiak, R.; Musial, J.; Frankowski, R.; Spychala, M.; Mielcarek, J.; Dobosz, B.; Krzyminiewski, R.; Sikorski, M.; Bendzinska-Berus, W.; Tykarska, E.; et al. Phthalocyanine-Grafted Titania Nanoparticles for Photodegradation of Ibuprofen. *Catalysts* **2020**, *10*, 1328. [CrossRef]
21. Li, K.; Pang, Y.; Lu, Q. In Situ Growth of Copper(II) Phthalocyanine-Sensitized Electrospun Ceo2/Bi2moo6 Nanofibers: A Highly Efficient Photoelectrocatalyst Towards Degradation of Tetracycline. *Inorg. Chem. Front.* **2019**, *6*, 3215–3224. [CrossRef]
22. Murphy, S.; Saurel, C.; Morrissey, A.; Tobin, J.; Oelgemoller, M.; Nolan, K. Photocatalytic Activity of a Porphyrin/TiO_2 Composite in the Degradation of Pharmaceuticals. *Appl. Catal. B-Environ.* **2012**, *119*, 156–165. [CrossRef]
23. Huang, X.; Groves, J.T. Oxygen Activation and Radical Transformations in Heme Proteins and Metalloporphyrins. *Chem. Rev.* **2018**, *118*, 2491–2553. [CrossRef]
24. Pereira, M.M.; Dias, L.D.; Calvete, M.J.F. Metalloporphyrins: Bioinspired Oxidation Catalysts. *Acs Catal.* **2018**, *8*, 10784–10808. [CrossRef]
25. Dubey, K.D.; Shaik, S. Cytochrome P450-the Wonderful Nanomachine Revealed through Dynamic Simulations of the Catalytic Cycle. *Acc. Chem. Res.* **2019**, *52*, 389–399. [CrossRef]
26. Larson, V.A.; Battistella, B.; Ray, K.; Lehnert, N.; Nam, W. Iron and Manganese Oxo Complexes, Oxo Wall and Beyond. *Nat. Rev. Chem.* **2020**, *4*, 404–419. [CrossRef]
27. Chino, M.; Leone, L.; Zambrano, G.; Pirro, F.; D'Alonzo, D.; Firpo, V.; Aref, D.; Lista, L.; Maglio, O.; Nastri, F.; et al. Oxidation Catalysis by Iron and Manganese Porphyrins within Enzyme-Like Cages. *Biopolymers* **2018**, *109*, e23107. [CrossRef] [PubMed]
28. Calvete, M.J.F.; Piñeiro, M.; Dias, L.D.; Pereira, M.M. Hydrogen Peroxide and Metalloporphyrins in Oxidation Catalysis: Old Dogs with Some New Tricks. *ChemCatChem* **2018**, *10*, 3615–3635. [CrossRef]
29. Zanatta, L.; Barbosa, I.; Filho, P.; Zanardi, F.; Bolzon, L.; Serra, O.; Iamamoto, Y. Metalloporphyrins in Drug and Pesticide Catalysis as Powerful Tools to Elucidate Biotransformation Mechanisms. *Mini-Rev. Org. Chem.* **2016**, *13*, 281–288. [CrossRef]
30. Walsh, C. *Antibiotics: Actions, Origins, Resistance*; ASM Press: Washington, DC, USA, 2003.

31. He, Y.; Huang, Z.; Ma, Z.; Yao, B.; Liu, H.; Hu, L.; Zhao, Q.; Yang, Q.; Liu, D.; Du, D. Highly Efficient Photocatalytic Performance and Mechanism of A-Zntcpc/G-C3n4 Composites for Methylene Blue and Tetracycline Degradation under Visible Light Irradiation. *Appl. Surf. Sci.* **2019**, *498*, 143834. [CrossRef]
32. Wang, X.; Song, Y.; Li, F.; Xu, W.; Zheng, Y.; Xu, L. A "Concentration-Induced Self-Assembly" Strategy for $AG_XH_{3-X}PMo_{12}O_{40}$ Nanorods: Synthesis, Photoelectric Properties and Photocatalytic Applications. *Nanoscale Adv.* **2021**, *3*, 446–454. [CrossRef]
33. Liu, C.; Cui, X.; Li, Y.; Duan, Q. A Hybrid Hollow Spheres Cu2o@Tio2-G-Zntapc with Spatially Separated Structure as an Efficient and Energy-Saving Day-Night Photocatalyst for Cr(VI) Reduction and Organic Pollutants Removal. *Chem. Eng. J.* **2020**, *399*, 125807. [CrossRef]
34. Jafarizadeh, T.; Hayati, P.; Neyrizi, H.Z.; Mehrabadi, Z.; Farjam, M.H.; Gutiérrez, A.; Adarsh, N.N. Synthesis and Structural Characterization of a Novel Zn(II) Metal Organic Complex (Zn-Moc) and Elimination of Highly Consumed Antibiotic; Tetracycline from Aqueous Solution by Their Nanostructures Photocatalyst under Visible Light. *J. Mol. Struct.* **2021**, *1228*, 129448. [CrossRef]
35. Zhao, S.; Li, S.; Zhao, Z.; Su, Y.; Long, Y.; Zheng, Z.; Cui, D.; Liu, Y.; Wang, C.; Zhang, X.; et al. Microwave-Assisted Hydrothermal Assembly of 2d Copper-Porphyrin Metal-Organic Frameworks for the Removal of Dyes and Antibiotics from Water. *Environ. Sci. Pollut. Res.* **2020**, *27*, 39186–39197. [CrossRef] [PubMed]
36. Yao, B.; Peng, C.; He, Y.; Zhang, W.; Zhang, Q.; Zhang, T. Conjugated Microspheres FeTCPP–TDI–TiO_2 with Enhanced Photocatalytic Performance for Antibiotics Degradation under Visible Light Irradiation. *Catal. Lett.* **2016**, *146*, 2543–2554. [CrossRef]
37. Yin, S.; Chen, Y.; Hu, Q.; Li, M.; Ding, Y.; Shao, Y.; Di, J.; Xia, J.; Li, H. In-Situ Preparation of Iron(II) Phthalocyanine Modified Bismuth Oxybromide with Enhanced Visible-Light Photocatalytic Activity and Mechanism Insight. *Colloids Surf. A Physicochem. Eng. Asp.* **2019**, *575*, 336–345. [CrossRef]
38. Sun, Y.; Feng, X.; Fu, S. Application of Response Surface Methodology for Optimization of Oxytetracycline Hydrochloride Degradation Using Hydrogen Peroxide/Polystyrene-Supported Iron Phthalocyanine Oxidation Process. *Water Sci. Technol.* **2020**, *81*, 1308–1318. [CrossRef] [PubMed]
39. Yao, B.H.; Peng, C.; He, Y.Q.; Zhang, W.; Yu, Y.; Zhang, T. Preparation and Visible-Light Photocatalytic Activity of FeTPP-CR-TiO_2 Microspheres. *J. Chem. Phys.* **2016**, *29*, 717–724. [CrossRef]
40. Jia, H.; Ma, D.; Zhong, S.; Li, L.; Li, L.; Xu, L.; Li, B. Boosting Photocatalytic Activity under Visible-Light by Creation of PCN-222/g-C3N4 Heterojunctions. *Chem. Eng. J.* **2019**, *368*, 165–174. [CrossRef]
41. Li, L.; Yu, X.; Xu, L.; Zhao, Y. Fabrication of a Novel Type Visible-Light-Driven Heterojunction Photocatalyst: Metal-Porphyrinic Metal Organic Framework Coupled with PW_{12}/TiO_2. *Chem. Eng. J.* **2020**, *386*, 123955. [CrossRef]
42. He, Y.; Lv, H.; Daili, Y.; Yang, Q.; Junior, L.B.; Liu, D.; Liu, H.; Ma, Z. Construction of a New Cascade Photogenerated Charge Transfer System for the Efficient Removal of Bio-Toxic Levofloxacin and Rhodamine B from Aqueous Solution: Mechanism, Degradation Pathways and Intermediates Study. *Environ. Res.* **2020**, *187*, 109647. [CrossRef] [PubMed]
43. Vignesh, K.; Rajarajan, M.; Suganthi, A. Photocatalytic Degradation of Erythromycin under Visible Light by Zinc Phthalocyanine-Modified Titania Nanoparticles. *Mater. Sci. Semicond. Process.* **2014**, *23*, 98–103. [CrossRef]
44. Li, N.; Lu, P.; He, C.; Lu, W.; Chen, W. Catalytic Degradation of Sulfaquinoxalinum by Polyester/Poly-4-Vinylpyridine Nanofibers-Supported Iron Phthalocyanine. *Environ. Sci. Pollut. Res.* **2018**, *25*, 5902–5910. [CrossRef] [PubMed]
45. Keşir, M.K.; Sökmen, M.; Bıyıklıoğlu, Z. Photocatalytic Efficiency of Metallo Phthalocyanine Sensitized TiO_2 (MPc/TiO_2) Nanocomposites for Cr(VI) and Antibiotic Amoxicillin. *Water* **2021**, *13*, 2174. [CrossRef]
46. Feng, D.; Gu, Z.-Y.; Li, J.-R.; Jiang, H.-L.; Wei, Z.; Zhou, H.-C. Zirconium-Metalloporphyrin PCN-222: Mesoporous Metal–Organic Frameworks with Ultrahigh Stability as Biomimetic Catalysts. *Angew. Chem. Int. Ed.* **2012**, *51*, 10307–10310. [CrossRef] [PubMed]
47. Almeida Lage, A.L.; Moreira Meireles, A.; Capelão Marciano, A.; Martins Ribeiro, J.; de Souza-Fagundes, E.M.; Carvalho da Silva Martins, D. Ciprofloxacin Degradation by First-, Second-, and Third-Generation Manganese Porphyrins. *J. Hazard. Mater.* **2018**, *360*, 445–451. [CrossRef]
48. Lage, A.L.A.; Marciano, A.C.; Venâncio, M.F.; da Silva, M.A.N.; Martins, D.C.d.S. Water-Soluble Manganese Porphyrins as Good Catalysts for Cipro- and Levofloxacin Degradation: Solvent Effect, Degradation Products and Dft Insights. *Chemosphere* **2021**, *268*, 129334. [CrossRef]
49. Meireles, A.M.; Almeida Lage, A.L.; Ribeiro, J.M.; Silva, M.A.N.d.; Souza-Fagundes, E.M.d.; Martins, D.C.d.S. Synthetic Mn(Iii) Porphyrins as Biomimetic Catalysts of Cyp450: Degradation of Antibiotic Norfloxacin in Aqueous Medium. *Environ. Res.* **2019**, *177*, 108615. [CrossRef] [PubMed]
50. De Souza Santos, L.V.; Lebron, Y.A.R.; Moreira, V.R.; Jacob, R.S.; Martins, D.C.d.S.; Lange, L.C. Norfloxacin and Gentamicin Degradation Catalyzed by Manganese Porphyrins under Mild Conditions: The Importance of Toxicity Assessment. *Environ. Sci. Pollut. Res.* 2021. [CrossRef]
51. Zhang, Y.; Li, H.; Huang, H.; Zhang, Q.; Guo, Q. Graphene Oxide Supported Cobalt Phthalocyanine as Heterogeneous Catalyst to Activate Peroxymonosulfate for Efficient Degradation of Norfloxacin Antibiotics. *J. Environ. Eng.* **2018**, *144*, 04018052. [CrossRef]
52. Sun, Y.; Zheng, W.; Fu, S.; Singh, R.P. Immobilization of Iron Phthalocyanine on 4-Aminopyridine Grafted Polystyrene Resin as a Catalyst for Peroxymonosulfate Activation in Eliminating Tetracycline Hydrochloride. *Chem. Eng. J.* **2020**, *391*, 123611. [CrossRef]
53. Zhu, Z.; Lu, W.; Li, N.; Xu, T.; Chen, W. Pyridyl-Containing Polymer Blends Stabilized Iron Phthalocyanine to Degrade Sulfonamides by Enzyme-Like Process. *Chem. Eng. J.* **2017**, *321*, 58–66. [CrossRef]

54. Piccirillo, G.; Moreira-Santos, M.; Válega, M.; Eusébio, M.E.S.; Silva, A.M.S.; Ribeiro, R.; Freitas, H.; Pereira, M.M.; Calvete, M.J.F. Supported Metalloporphyrins as Reusable Catalysts for the Degradation of Antibiotics: Synthesis, Characterization, Activity and Ecotoxicity Studies. *Appl. Catal. B Environ.* **2021**, *282*, 119556. [CrossRef]
55. Nackiewicz, J.; Kolodziej, L.; Poliwoda, A.; Broda, M.A. Oxidation of Diclofenac in the Presence of Iron(II) Octacarboxyphthalocyanine. *Chemosphere* **2021**, *265*, 129145. [CrossRef] [PubMed]
56. Barros, W.R.P.; Borges, M.P.; Steter, J.R.; Forti, J.C.; Rocha, R.S.; Lanza, M.R.V. Degradation of Dipyrone by Electrogenerated H_2O_2 Combined with Fe^{2+} Using a Modified Gas Diffusion Electrode. *J. Electrochem. Soc.* **2014**, *161*, H867–H873. [CrossRef]
57. Sułek, A.; Pucelik, B.; Kuncewicz, J.; Dubin, G.; Dąbrowski, J.M. Sensitization of Tio2 by Halogenated Porphyrin Derivatives for Visible Light Biomedical and Environmental Photocatalysis. *Catal. Today* **2019**, *335*, 538–549. [CrossRef]
58. Wang, S.L.; Ma, W.H.; Jia, M.K.; Huang, Y.P. Degradation of Pollutants by Hydrophobic FePCCl16 under Ultraviolet and Visible Light. *Fresenius Environ. Bull.* **2013**, *22*, 549–555.
59. Qian, H.; Yu, G.; Hou, Q.; Nie, Y.; Bai, C.; Bai, X.; Wang, H.; Ju, M. Ingenious Control of Adsorbed Oxygen Species to Construct Dual Reaction Centers Zno@Fepc Photo-Fenton Catalyst with High-Speed Electron Transmission Channel for Ppcps Degradation. *Appl. Catal. B Environ.* **2021**, *291*, 120064. [CrossRef]
60. Gao, Y.X.; Xia, J.; Liu, D.C.; Kang, R.X.; Yu, G.; Deng, S.B. Synthesis of Mixed-Linker Zr-Mofs for Emerging Contaminant Adsorption and Photodegradation under Visible Light. *Chem. Eng. J.* **2019**, *378*, 122118. [CrossRef]
61. Gao, Y.X.; Lu, J.; Xia, J.; Yu, G. In Situ Synthesis of Defect-Engineered Mofs as a Photoregenerable Catalytic Adsorbent: Understanding the Effect of Lml, Adsorption Behavior, and Photoreaction Process. *ACS Appl. Mater. Interfaces* **2020**, *12*, 12706–12716. [CrossRef]
62. Wu, M.H.; Fu, K.; Deng, H.P.; Shi, J. Cobalt Tetracarboxyl Phthalocyanine-Manganese Octahedral Molecular Sieve (OMS-2) as a Heterogeneous Catalyst of Peroxymonosulfate for Degradation of Diclofenac. *Chemosphere* **2019**, *219*, 756–765. [CrossRef]
63. Chapman, C.M.; Pruneau, J.M.; Laverack, C.A.; Dutton, A.S.; Jones, G.B. Biomimetic Oxidation of Acetaminophen Prodrugs Catalyzed by Iron Porphyrins: Effect of Nitrogen and Thiolate Axial Ligands on Drug and Metabolite Formation. *Appl. Catal. A Gen.* **2016**, *510*, 204–215. [CrossRef]
64. Wang, L.; Lu, W.; Ni, D.; Xu, T.; Li, N.; Zhu, Z.; Chen, H.; Chen, W. Solar-Initiated Photocatalytic Degradation of Carbamazepine on Excited-State Hexadecachlorophthalocyanine in the Presence of Peroxymonosulfate. *Chem. Eng. J.* **2017**, *330*, 625–634. [CrossRef]
65. Xu, T.; Ni, D.; Chen, X.; Wu, F.; Ge, P.; Lu, W.; Hu, H.; Zhu, Z.; Chen, W. Self-Floating Graphitic Carbon Nitride/Zinc Phthalocyanine Nanofibers for Photocatalytic Degradation of Contaminants. *J. Hazard. Mater.* **2016**, *317*, 17–26. [CrossRef] [PubMed]
66. Xu, T.; Wang, D.; Dong, L.; Shen, H.; Lu, W.; Chen, W. Graphitic Carbon Nitride Co-Modified by Zinc Phthalocyanine and Graphene Quantum Dots for the Efficient Photocatalytic Degradation of Refractory Contaminants. *Appl. Catal. B Environ.* **2019**, *244*, 96–106. [CrossRef]
67. Wu, F.; Huang, H.; Xu, T.; Lu, W.; Li, N.; Chen, W. Visible-Light-Assisted Peroxymonosulfate Activation and Mechanism for the Degradation of Pharmaceuticals over Pyridyl-Functionalized Graphitic Carbon Nitride Coordinated with Iron Phthalocyanine. *Appl. Catal. B Environ.* **2017**, *218*, 230–239. [CrossRef]
68. Dong, L.; Xu, T.; Chen, W.; Lu, W. Synergistic Multiple Active Species for the Photocatalytic Degradation of Contaminants by Imidazole-Modified g-C3N4 Coordination with Iron Phthalocyanine in the Presence of Peroxymonosulfate. *Chem. Eng. J.* **2019**, *357*, 198–208. [CrossRef]
69. Zhu, Z.; Lu, W.; Xu, T.; Li, N.; Wang, G.; Chen, W. High-Valent Iron-Oxo Complexes as Dominant Species to Eliminate Pharmaceuticals and Chloride-Containing Intermediates by the Activation of Peroxymonosulfate under Visible Irradiation. *Catal. Lett.* **2020**, *150*, 1355–1367. [CrossRef]
70. Zhu, Z.; Chen, Y.; Gu, Y.; Wu, F.; Lu, W.; Xu, T.; Chen, W. Catalytic Degradation of Recalcitrant Pollutants by Fenton-Like Process Using Polyacrylonitrile-Supported Iron (II) Phthalocyanine Nanofibers: Intermediates and Pathway. *Water Res.* **2016**, *93*, 296–305. [CrossRef]
71. Zhou, J.; Wu, F.; Zhu, Z.; Xu, T.; Lu, W. Identification of O-Bridge Iron Perfluorophthalocyanine Dimer and Generation of High-Valent Diiron-Oxo Species for the Oxidation of Organic Pollutants. *Chem. Eng. J.* **2017**, *328*, 915–926. [CrossRef]
72. Zhao, Z.; Zhou, M.; Li, N.; Yao, Y.; Chen, W.; Lu, W. Degradation of Carbamazepine by MWCNTs-Promoted Generation of High-Valent Iron-Oxo Species in a Mild System with O-Bridged Iron Perfluorophthalocyanine Dimers. *J. Environ. Sci.* **2021**, *99*, 260–266. [CrossRef]
73. Kruid, J.; Fogel, R.; Limson, J. Unsubstituted Metallophthalocyanine Catalysts for the Removal of Endocrine Disrupting Compounds Using H_2O_2 as Oxidant. *Environ. Sci. Pollut. Res.* **2018**, *25*, 32346–32357. [CrossRef] [PubMed]
74. Fernandez, L.; Borzecka, W.; Lin, Z.; Schneider, R.J.; Huvaere, K.; Esteves, V.I.; Cunha, A.; Tome, J.P.C. Nanomagnet-Photosensitizer Hybrid Materials for the Degradation of 17 Beta-Estradiol in Batch and Flow Modes. *Dyes Pigm.* **2017**, *142*, 535–543. [CrossRef]
75. Savitha, R.; Raghunathan, R.; Nolan, K.; Morrissey, A.; Selvam, P.; Chetty, R. Evaluation of Visible-Light Driven Photocatalytic Reaction by Porphyrin Coupled TiO_2 Nanotubes Obtained Via Rapid Breakdown Anodization. *J. Environ. Chem. Eng.* **2020**, *8*, 104382. [CrossRef]

76. Neves, C.M.B.; Filipe, O.M.S.; Mota, N.; Santos, S.A.O.; Silvestre, A.J.D.; Santos, E.B.H.; Neves, M.G.P.M.S.; Simões, M.M.Q. Photodegradation of Metoprolol Using a Porphyrin as Photosensitizer under Homogeneous and Heterogeneous Conditions. *J. Hazard. Mater.* **2019**, *370*, 13–23. [CrossRef] [PubMed]
77. Minhui, W.; Jun, S.; Chao, D.; Huiping, D. Binuclear Cobalt Phthalocyanine Supported on Manganese Octahedral Molecular Sieve: High-Efficiency Catalyzer of Peroxymonosulfate Decomposition for Degrading Propranolol. *Sci. Total Environ.* **2019**, *686*, 97–106. [CrossRef]